

# Quantifying the Dynamics of Innovation Abandonment Across Scientific, Technological, Commercial, and Pharmacological Domains

Binglu Wang<sup>1,2,3\*</sup>, Ching Jin<sup>1,2,3,4\*</sup>, Chaoming Song<sup>5</sup>, Johannes Bjelland<sup>6</sup>, Brian Uzzi<sup>1,2,3</sup> & Dashun Wang<sup>1,2,3†</sup>

<sup>1</sup> *Center for Science of Science and Innovation, 600 Foster Street, Evanston, IL 60208, USA*

<sup>2</sup> *Northwestern Institute on Complex Systems (NICO), 600 Foster Street, Evanston, IL 60208, USA*

<sup>3</sup> *Kellogg School of Management, 2211 Campus Dr, Evanston, IL 60208, USA*

<sup>4</sup> *Centre for Interdisciplinary Methodologies, University of Warwick, Coventry, CV4 7AL, United Kingdom*

<sup>5</sup> *Department of Physics, University of Miami, 1320 S Dixie Hwy, Coral Gables, FL 33146, USA*

<sup>6</sup> *Telenor Research and Development, Snarøyveien 30 N-1360 Fornebu, Norway*

\* *These authors contributed equally to the work.*

† *Correspondence should be addressed to D.W. ([dashun.wang@northwestern.edu](mailto:dashun.wang@northwestern.edu))*

**Despite the vast literature on the diffusion of innovations that impacts a broad range of disciplines, our understanding of the abandonment of innovations remains limited yet is essential for a deeper understanding of the innovation lifecycle. Here, we analyze four large-scale datasets that capture the temporal and structural patterns of innovation abandonment across scientific, technological, commercial, and pharmacological domains. The paper makes three primary contributions. First, across these diverse domains, we uncover one simple pattern of preferential abandonment, whereby the probability for individuals or organizations to abandon an innovation increases with time and correlates with the number of network neighbors who have abandoned the innovation. Second, we find that the presence of preferential abandonment fundamentally alters the way in which the underlying ecosystem breaks down, inducing a novel structural collapse in networked systems commonly perceived as robust against abandonments. Third, we derive an analytical framework to systematically understand the impact of preferential abandonment on network dynamics, pinpointing specific conditions where it may accelerate, decelerate, or have an identical effect compared to random abandonment, depending on the network topology. Together, these results deepen our quantitative understanding of the abandonment of innovation within networked social systems, with implications for the robustness and functioning of innovation communities. Overall, they demonstrate that the dynamics of**

**innovation abandonment follow simple yet reproducible patterns, suggesting that the uncovered preferential abandonment may be a generic property of the innovation lifecycle.**

Popularized in its contemporary form by Rogers [1], but with roots tracing back to Bernoulli [2] in the eighteenth century, the studies of diffusion of innovations have transformed our understanding of how innovations spread among interacting agents, impacting a diverse range of domains from science [3-7] and technology [8-10] to epidemiology [11-14] to social systems [15-24]. A fundamental property of an innovation's lifecycle is that its popularity eventually decays with time [25-32]. While our understanding of the diffusion of innovations grows, the counterpart of this process—the abandonment of innovations—has received relatively little attention, leaving open important questions regarding the dynamics of innovation abandonment.

Indeed, a fundamental tension between the social and computational literature concerns the rate of abandonment over an innovation's lifecycle. On the one hand, the prevailing computational frameworks in modeling abandonment typically rely on models from epidemiology, sharing the common assumption that abandoning processes follow Poissonian dynamics, predicting a constant rate of abandonment over time [11, 14, 33-40]. This Poissonian assumption is consistent with the fact that innovations tend to have a typical lifespan, and has shown initial success in capturing the substitution dynamics between successive generations of innovations [37]. On the other hand, theories in the social sciences substantially challenge this Poissonian assumption. For instance, research on network externality and social influence [16-18, 20, 41-44] suggests that individual actions of abandonment may be affected by the choices of others in the social network. Along these lines of inquiry, the literature posits that the abandonment of innovations may closely mirror the adoption process, which is commonly characterized by preferential attachment [3, 4, 45]. Yet at the same time, there are reasons to believe that abandonment may follow different dynamics than the adoption process, in part because prior to abandonment, agents have had direct information and experience with the innovation or practice [26, 46, 47], potentially reducing their susceptibility to external factors.

These contrasting perspectives highlight the fact that, despite the ubiquitous nature of abandonment across innovation domains and the multidisciplinary interests in understanding abandonment dynamics [31, 43, 46-49], it has remained elusive to collect large-scale datasets that systematically capture the temporal and structural patterns governing innovation abandonment. Here we understand abandonment to be the act of giving up an idea or stopping an activity with a

high likelihood of not returning to it. To this end, we assemble and analyze large-scale datasets across four distinct domains, tracing the innovation lifecycles from adoption to abandonment.

The first dataset ( $D_1$ ) captures the abandonment dynamics of scientific fields as scientists shift their focus out of certain areas of research. Here we use the Microsoft Academic Graph data [50] to measure the fraction of publishing scientists in each field over time, allowing us to delineate the lifecycle of 1219 scientific fields from 1940 to 2015 and quantify the dynamics of scientists leaving a field (SI S1.1). Our second dataset ( $D_2$ ) records the dynamics of inventors shifting across patenting domains. Specifically,  $D_2$  captures 6.9M patents granted by the USPTO from 1976 to 2015. Similar to  $D_1$ , here we trace the lifecycles of 291 patenting domains, approximated by Cooperative Patent Classification codes (CPC), and measure the proportion of inventors in each domain over time (SI S1.2). Our third dataset ( $D_3$ ) focuses on a commercial domain and traces the individual usage history of mobile handsets within a European country (704 types of handsets by 3.5M users), allowing us to quantify the abandonment dynamics of mobile handsets through the changes in daily active users over a period of nine years (2006-2014) (SI S1.3). Lastly, we construct our fourth dataset ( $D_4$ ) tracing the dynamics of pharmacological innovations, and analyze the abandonment of drug mechanisms, i.e., biological mechanisms of actions or MOAs, as pharmaceutical organizations shift their focus on certain MOAs in drug development. Here we use the Cortellis Drug Discovery Intelligence database, which contains the largest and most comprehensive drug development records in the world, covering 648,702 drugs over the past 25 years [51, 52]. To quantify the abandonment dynamics of pharmacological innovations, we examine MOAs associated with each drug and measure the R&D focus of pharmaceutical companies on these MOAs. In total, we trace 248 MOAs by 5,133 pharmaceutical companies and measure the fraction of companies using each MOAs in drug development (SI S1.4).

Figure 1ADGJ plot the popularity dynamics of different scientific fields, patenting domains, mobile handsets, and drug's mechanisms of action, respectively. All four domains exhibit a similar rise-and-fall pattern, demonstrating both the adoption and abandonment processes are important for understanding the innovation lifecycle. Here we focus on the declining phase of each innovation and measure the rate of abandonment  $\nu$  as a function of time ( $t$ ). We find that, across scientific fields, patenting domains, mobile handsets, and drug MOAs, the average abandonment probability ( $\nu$ ) systematically increases with time ( $t$ ) (Fig. 1BEHK). Going beyond the aggregate



estimates, we test if the observed trend holds for individual scientific fields, patenting domains, mobile handsets or drug MOAs. In particular, for each innovation, we build panel data containing all of its users, fit this panel data using linear regression, and estimate the slope of the fit for each innovation, to approximate how its abandonment rate changes as a function of time (Fig. 1CFIL). We find that the majority of scientific fields (98.11%), patenting domains (92.28%), mobile handsets (91.57%) and drug MOAs (84.91%) can be approximated by a positive slope, suggesting the abandonment probability of different innovations appears to trend upward in a rather ubiquitous manner.

The results in Fig. 1 contest the Poissonian assumption, showing that the rate of innovation abandonment tends to increase over time rather than stay constant. Yet at the same time, these results conflate temporal and structural effects, raising the question of whether the patterns observed in Fig. 1 can be simply explained by the temporal obsolescence of innovations, or whether there is any structural effect associated with the underlying network that goes beyond the temporal effect. To answer this question, we collect further data to approximate the underlying network behind each of our four datasets. More specifically, for  $D_1$  and  $D_2$ , we construct the collaboration network using co-authorship and co-inventor information, respectively [53]. For  $D_3$ , we collect anonymous phone call records among 1.7M users within a three-month period (October 1, 2013-January 1, 2014), to approximate the social network among a subset of users. And for  $D_4$ , we calculate the similarity in market focus among pharmaceutical companies to approximate the underlying proximity between two companies through their shared similarity in market focus. Together, these additional datasets offer us an opportunity to further examine the social context in which the abandonment processes unfold.

To understand the correlation between abandonment rate and network structure, we first control for potential temporal effects by restricting our measurement within a short time interval (S2). For each innovation  $i$ , we separate its users in our datasets into two groups, based on whether or not abandonments of innovation  $i$  have occurred among their network neighbors ( $r_i > 0$  vs.  $r_i = 0$ ), and measure the rate of abandonment separately for the two groups. We find that the distributions of abandonment rates for the two groups show visibly different patterns (Fig. 2ABCD), with the distribution for the first group ( $r_i > 0$ ) shifting systematically to the right of the  $r_i = 0$  group. These findings suggest that the abandonment rate tends to be higher when abandonment events

have occurred among an individual's network neighbors. We then test whether the abandonment probability ( $v_i$ ) increases with the number of network neighbors who have also abandoned the innovation ( $r_i$ ). Figure 2EFGH show four case studies, where we measure the rate of abandonment as a function of  $r_i$  for one selected example in each dataset. Across these four cases,  $v_i$  shows a positive relationship with  $r_i$ , indicating that the abandonment probability appears to increase with the number of network neighbors who have abandoned the innovation. By contrast, in a null model of random abandonment,  $v_i$  is independent of  $r_i$  (Fig. 2EFGH, grey dashed line). To systematically test across different innovations in different domains, we fit the relationship between  $v_i$  and  $r_i$  for each scientific field, patenting domain, mobile handset, and drug MOAs, respectively, with a linear ansatz for all of its users, finding that a substantial fraction of scientific, technological, commercial and pharmacological innovations can be approximated by a positive slope (73.21%, 70.4%, 79.34%, and 69.86%, respectively) (Fig. 2IJKL).

Taken together, these results suggest that the growth in the rate of abandonment over time is not simply due to temporal effects; rather, the abandonment dynamics appear to correlate with the number of network neighbors who have abandoned the innovation. Overall, these results empirically demonstrate a preferential abandonment phenomenon, confronting the prevailing computational frameworks in modeling abandonment dynamics. Most importantly, the patterns of preferential abandonment appear rather universal across the scientific, technological, commercial, and pharmacological domains we studied. Indeed, the four innovation domains differ substantially in their scope, scale, temporal resolution, and nature of the innovation itself. Yet despite these clear differences, and the myriad factors that might affect the decisions of individuals and organizations to abandon an innovative pursuit [31, 43, 46-49], the patterns of preferential abandonment show remarkable consistencies across these rather diverse domains.

The concept of preferential abandonment intersects with several important ideas in social science, from peer effects and network externality [16, 20, 41-44] to the theory of creative destruction [54] to vacancy chains [47, 55]. However, it challenges the traditional computational models, which predominantly posit that abandonment follows Poissonian dynamics [11, 14, 33-40]. This prompts us to explore this phenomenon further through a computational perspective, asking: How does the dynamic of a system alter when its decline adheres to preferential abandonment?

Interestingly, the phenomenon of preferential abandonment during an innovation’s declining phase seems to mirror the preferential attachment process, commonly responsible for the growth phase of an innovation community. This observation prompts us to explore the effects of preferential abandonment on networked systems, whose growth is typically governed by preferential attachment. Preferential attachment is a cornerstone concept in network science [56, 57], being the key ingredient for generating scale-free networks with heterogeneous degree distributions, which are known for their resilience against random node removals [58-60]. Empirical analyses of declining networks also suggest that a network may further retain its robustness during disassembly through partial recovery and the preservation of asymmetric links [26]. Therefore, the prevailing evidence implies that for innovation communities that grew through preferential attachment, one would expect these communities to be robust against abandonment, retaining their main connectivity and functionality despite declining memberships. However, as we show next, the presence of preferential abandonment fundamentally alters the way in which networked systems break down, inducing a novel structural collapse in ecosystems that were previously considered robust against abandonment.

To understand the structural consequences of preferential abandonment, we consider a preferential abandonment process on a scale-free network with  $N$  nodes. In each time step, nodes are removed with probability:

$$v_i = v_0[\alpha r_i + (1 - \alpha)]. \quad (1)$$

Here, we denote with  $r_i$  the number of nodes that have already been removed among the neighbors of node  $i$  (i.e., those who have abandoned the innovation), and  $\alpha$  captures the strength of preferential abandonment. When  $\alpha = 0$ , nodes are removed randomly with the same probability  $v_0$ , and (1) recovers the existing modeling framework of abandonment dynamics, following the random abandonment process. We first simulate the abandonment process on a scale-free network ( $P_k \sim k^{-\gamma}$ ) with  $\gamma = 2.5$ , for both random abandonment ( $\alpha = 0$ ) and preferential abandonment ( $\alpha = 0.5$ ). We trace the size of the giant component ( $S$ ) as a function of the fraction of nodes removed ( $f$ ). We find that, under random abandonment (Fig. 3A, blue line), the network shows a high degree of robustness [11, 14, 58], as its giant connected component maintains its integrity even after a large fraction of nodes has been removed. If, however, the system undergoes

preferential abandonment (Fig. 3A, yellow line), a fundamentally different pattern emerges. First, conditional on removing the same number of nodes, the network breaks down much more quickly than random abandonment. More importantly, the network appears to undergo a critical process and become fragmented even with a substantial fraction of nodes remaining in the system.

To understand these simulation results, we adopt the heterogeneous mean-field approximation (HMA) to analytically calculate the critical point ( $f_c$ ) under preferential abandonment through a self-consistent equation:

$$f_c = 1 - \frac{\langle k \rangle \sum_k P_k h(f_c)^k}{\sum_k P_k (k^2 - k) h(f_c)^{k-2}} = 1 - \frac{G_0(h(f_c)) \langle k \rangle}{G_0'(h(f_c))}, \quad (2)$$

where  $h$  satisfies the following differential equation:

$$\frac{dh}{df} = \frac{-\alpha h G_0^2(h) + \alpha G_0(h) G_1(h) (1-f)}{\alpha (1-f) h G_0(h) G_0'(h) - \alpha (1-f)^2 G_0'(h) G_1(h) + (1-\alpha)(1-f) G_0^2(h)}. \quad (3)$$

Here,  $G_0$  and  $G_1$  are generating functions of network degrees:  $G_0(x) \equiv \sum_k P_k x^k$  and  $G_1(x) \equiv \sum_k \frac{1}{\langle k \rangle} (k+1) P_{k+1} x^k$ . We find that in scale-free networks with  $\gamma < 3$ ,  $h(f)$  becomes less than 1 under preferential abandonment, leading to convergence in the factor  $\sum_k P_k (k^2 - k) h(f_c)^{k-2}$ . This indicates the existence of a critical point under preferential abandonment. Importantly, we find that, for any  $\alpha$  larger than 0,  $h(f)$  is always smaller than 1. This means, regardless of the strength of preferential abandonment (i.e., no matter how small  $\alpha$  is), we will always find a critical point  $f_c < 1$  satisfying (2). In other words, in the presence of preferential abandonment— independent of its magnitude—scale-free networks break down following fundamentally different dynamics, characterized by a phase transition that is absent in the random abandonment case.

To verify this theoretical prediction, we generate scale-free networks by varying their degree heterogeneity and simulate the preferential abandonment process with a given  $\alpha$  (Fig. 3D). Our simulation results show excellent agreement with our analytical calculations (Eq. 2) (Fig. 3D). Figure 3BC visualize the same scale-free network with half of the nodes removed ( $f = 0.5$ ) under random abandonment and preferential abandonment, respectively. While the two networks have the same number of nodes remaining, they show markedly different patterns. Whereas a giant

component composed of high-degree nodes persists under random abandonment (Fig. 3C), the giant component in the preferential abandonment case only contains a small number of low-degree nodes (Fig. 3B). This highlights the key difference between random and preferential abandonment. Whereas hubs maintain the robustness of the network under random abandonment, they become sources of fragility under preferential abandonment.

These results connect closely with the network science literature [11, 14, 26, 37, 56-71], which has extensively studied how networked systems collapse under the removal of nodes or links [58-62], ranging from random failures [11, 14, 59], to strategic [60] or degree-based attacks [67] to articulation points [68] and cascading failure [69-71]. In particular, the role of hubs as sources of fragility suggests a high-level similarity between preferential abandonment and attacks on networks [58-60] (Fig. 3D), raising the question of whether preferential abandonment is equivalent to attacks on a network. To answer this question, we examine preferential abandonment on Erdős-Rényi (ER) networks. The literature on network attacks [58, 60, 67] predicts an earlier onset of phase transition on the ER network (Fig. 3H, the black dashed line). Yet surprisingly, we find that in ER networks, preferential abandonment follows indistinguishable dynamics as random abandonment (Fig. 3H). The main intuition here is that, as the nodes in ER networks are connected randomly, there is no correlation between the number of abandoned neighbors ( $r$ ) of a node and its remaining degree. Therefore, targeting nodes with high  $r$  in ER network is equivalent to randomly removing nodes with any degree. Thus, preferential abandonment and random abandonment on ER networks follow identical dynamics (Fig. 3EFG), highlighting the highly non-trivial effects of preferential abandonment on network dynamics. Overall, while finite size effects prohibit us from directly testing these percolation processes on empirical data, our analytical results demonstrate that preferential abandonment induces novel critical dynamics in the breakdown of networks.

Next, we show that the key to unpacking these novel critical dynamics induced by preferential abandonment lies in the relationship between the number of abandonment neighbors ( $r$ ) of a node and its current degree ( $k_f$ ) after  $f$  fraction of nodes has abandoned, which varies for different network topologies. To see this, we first measure  $k_f$  vs  $r$  at different levels of  $f$  for a scale-free network (Fig. 4BC). We find that the two quantities follow an asymptotically linear relationship, suggesting that nodes with larger  $r$  are also characterized by a higher remaining degree, mimicking

the attack processes (see SI Fig. S5 for details). When we repeat the analyses on ER networks (Fig. 4E), however, we find that  $k_f(r)$  remains constant for any given  $r$  (Fig. 4F) under preferential abandonment, which is the same as random abandonment. While nodes with higher  $r$  are more likely to be selected under preferential abandonment, in the ER network, this process effectively selects nodes with random  $k_f$ , explaining why preferential abandonment on ER networks follows the same dynamics as random abandonment.

Our analytical results predict the asymptotic behavior of  $k_f(r)$  as  $r \rightarrow \infty$  follows

$$k_f(r) \sim (r + 1) \frac{P_k(r+1)}{P_k(r)}, \quad (4)$$

suggesting that this key relationship is governed by the original degree distribution of the network  $P(k)$  (Fig. 4CFI, also see SI S4 for details). Since any properly normalizable distribution requires  $\frac{P_k(r+1)}{P_k(r)} < 1$ , Eq. (4) predicts that asymptotically  $k_f(r)$  is bounded by a linear scaling. For any distribution with a tail fatter than or equal to the geometric distribution, e.g., the power law, it saturates to the linear scaling bound. However, for the Poisson degree  $P(k) \sim \frac{\lambda^k}{k!}$ , Eq. (4) predicts  $k_f \sim \lambda$ , converging to the average degree of the original network. Thus, the Poisson degree distribution serves as a key division here. If the degree distribution has a heavier tail than Poisson distribution, such as in power-law distributions,  $k_f$  increases with  $r$ . Hence, in such networks, hubs are more likely to be removed under preferential abandonment, leading to an earlier onset of the phase transition. By contrast, for networks with a narrower degree distribution than Poisson distribution, such as normal distributions (Fig. 4GHI), there is a negative correlation between  $k_f$  and  $r$ , where once nodes with higher  $r$  are removed, preferential abandonment actually targets nodes with lower current degree, thus inducing an even slower percolation than random abandonment. Table 1 summarizes the prediction of Eq. (4) for several common networks.

Table 1 Summary of different network structures

Network	Degree Distribution	$k_f(r) _{r \rightarrow \infty}$
scale-free networks	$k^{-\lambda}$	$r$

ER networks	$\frac{\lambda^k e^{-\lambda}}{k!}$	$\lambda$
Gaussian networks	$e^{-\frac{1}{2}\left(\frac{k-\mu}{\sigma}\right)^2}$	0

---

Taken together, this paper examines the abandoning dynamics across four distinct innovation domains and makes three primary contributions. First, it empirically documents a simple yet ubiquitous phenomenon of preferential abandonment governing the dynamics of innovation abandonment. We find that at the macro level, the rate of abandonment increases with time, influencing the overall popularity dynamics. Yet beneath this macro trend lies a simple effect of preferential abandonment, which governs the abandonment process. Second, we incorporate this empirical finding into our current modeling frameworks and find that the presence of preferential abandonment creates novel yet complex dynamics in the breakdown of the overall ecosystem, generating a new form of structural collapse in networked systems that are thought to be robust against random abandonments. Third, we derive an analytical framework to systematically understand the impact of preferential abandonment on network breakdown, pinpointing specific conditions where it may accelerate, decelerate, or have an identical effect compared to random abandonment, depending on the network topology. Overall, these results provide a new quantitative basis for understanding the abandonment of innovation within networked social systems, which has implications for the robustness and functioning of innovation communities.

While this paper synthesizes empirical evidence from four distinct domains to document the phenomenon of preferential abandonment and its impact on the disintegration of innovation communities, it is important to acknowledge a significant limitation: the study does not establish the origins of preferential abandonment, particularly regarding its potential interplay with preferential attachment. For example, it is possible that the observed preferential abandonment is an extension or byproduct of the preferential attachment mechanisms that govern the growth phase of the new communities. Although the findings of this paper remain valid irrespective of the specific origins of preferential abandonment, further research into the connections between the growth and decline of innovation communities could pave the way for a more integrated framework for understanding innovation life cycles, which would further the understanding and predictions of how innovation communities evolve and dissolve. Further, analyzing data across

four diverse domains, this paper mainly focuses on universal patterns that generalize across domains. At the same time, there exist substantial heterogeneities both within and across domains, representing fruitful directions for future work. Indeed, the variability in  $\alpha$  suggests that innovation has varying degrees of stickiness during abandonment. What factors tend to be associated with a higher or lower  $\alpha$  parameter? Beyond the universal patterns presented in this paper, insights into the heterogeneity in the abandonment processes may further our understanding of the potential mechanisms driving the dynamics of abandonment.

Overall, this paper demonstrates that the dynamics of innovation abandonment across scientific, technological, commercial, and pharmacological domains follow simple yet reproducible patterns, commonly governed by preferential abandonment. The phenomenon of preferential abandonment fundamentally alters the breakdown of innovation ecosystems, with implications for the robustness and functioning of the underlying systems. Curiously, preferential abandonment resembles behavior observed in a wide range of settings, including organization strategy [48, 49], culture [31], financial market [43], and healthcare [47], suggesting the concept of preferential abandonment may have broad relevance that goes beyond quoted examples.

### **Data Availability**

Scientific publication data used in this work is from Microsoft Academic Graph, where the raw data was publicly available at <https://www.microsoft.com/en-us/research/project/microsoft-academic-graph>. Patent data used in this work is from PatentsView, which is publicly available at <https://patentsview.org/download/data-download-tables>. Mobile phone data are not publicly available due to commercially sensitive information contained, but is available from the corresponding author on reasonable request. This work also uses drug data sourced from Cortellis, and researchers who wish to access raw data should contact the data sources directly. Data necessary for reproducing the main results will be available.

### **Code Availability**

The custom code used will be available.

### **Acknowledgement**



We thank all members of the Kellogg Center for Science of Science & Innovation (CSSI) and the Northwestern Institute on Complex System (NICO) for helpful discussions. D.W. is supported by the Air Force Office of Scientific Research under award numbers FA9550-17-1-0089 and FA9550-19-1-0354, National Science Foundation grant SBE 1829344, the Alfred P. Sloan Foundation G-2019-12485 and Peter G. Peterson Foundation 21048. The funders had no role in study design, data collection and analysis, decision to publish or preparation of the manuscript.

### **Author Contributions**

B.W., C.J., C.S., B.U., and D.W. designed the research; B.W. and C.J. collected data and conducted empirical and analytical analyses with help from D.W., C.S., J.B., B.U.; all authors discussed and interpreted results; B.W., C.J. and D.W. wrote the manuscript; all authors edited the manuscript.

### **Competing Interest Statement**

The authors declare no competing interests.

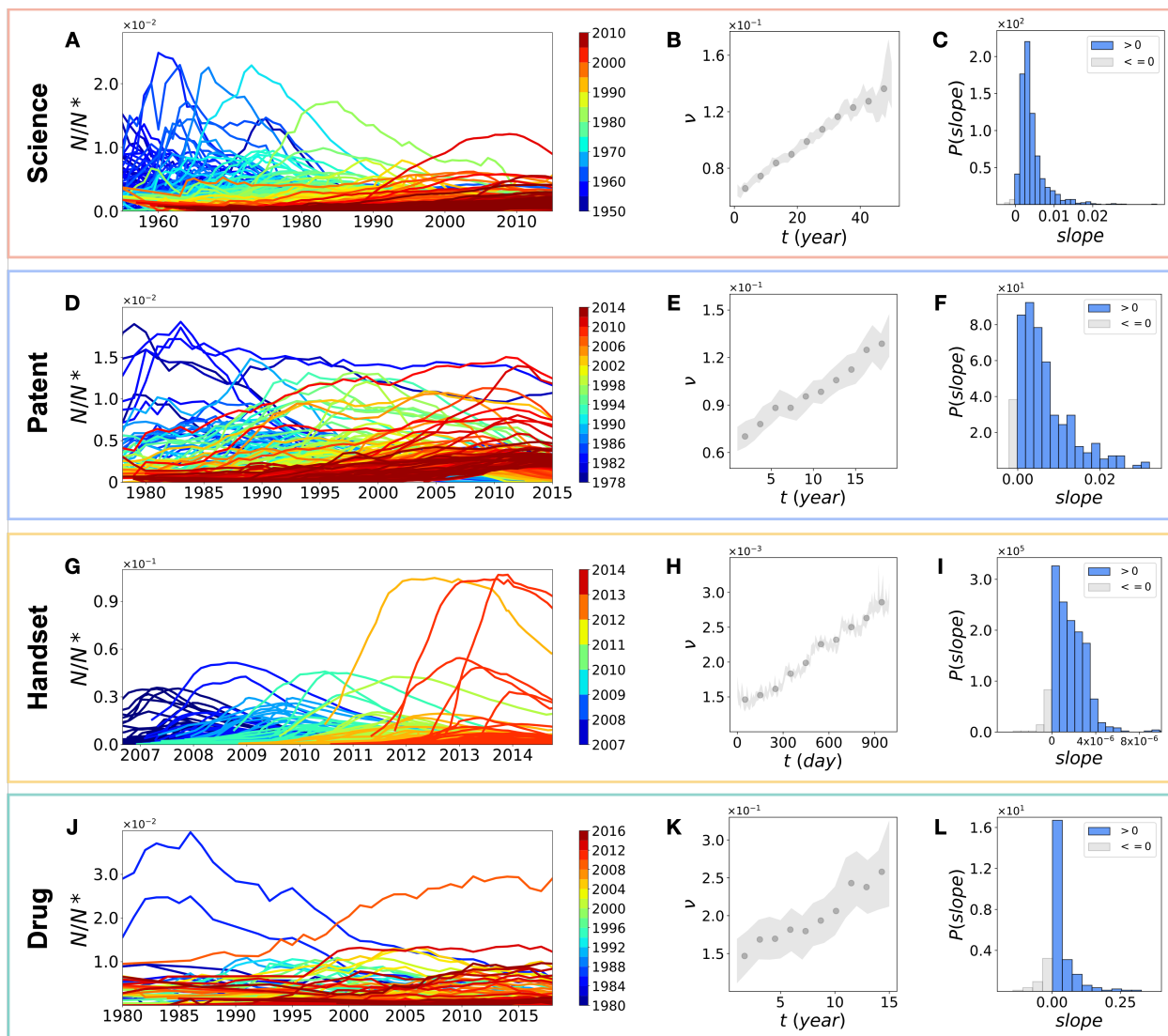


Figure 1: **Temporal dynamics of innovation abandonment.** (A, D, G, J) Popularity dynamics ( $\frac{N}{N^*}$ ) of scientific fields (A), patenting domains (D), mobile handsets (G) and drug MOAs (J). Here we calculate the proportion of scientists and inventors in each field, the ratio of active users for each mobile handset, and the fraction of pharmaceutical organizations focusing on each MOA. Each line represents a scientific field (A), patenting domain (D), handset type (G) or drug MOA (J). The color code corresponds to peak dates (when the population reaches to its maximum), shifting from blue to red. (B, E, H, K) The average abandonment probability  $\nu \equiv \frac{\Delta N^-}{N}$  as a function of time  $t$  for all scientific fields (B), patenting domains (E), mobile handsets (H) and drug MOAs (K), showing the abandoning rate on average increases with time. The shaded region represents a 95% confidence interval. (C, F, I, L) We estimate the relationship between the abandonment probability and time for individual scientific fields (C), patenting domains (F), mobile handsets (I) and drug MOAs (L) and plot the distributions of the estimated slope coefficients.

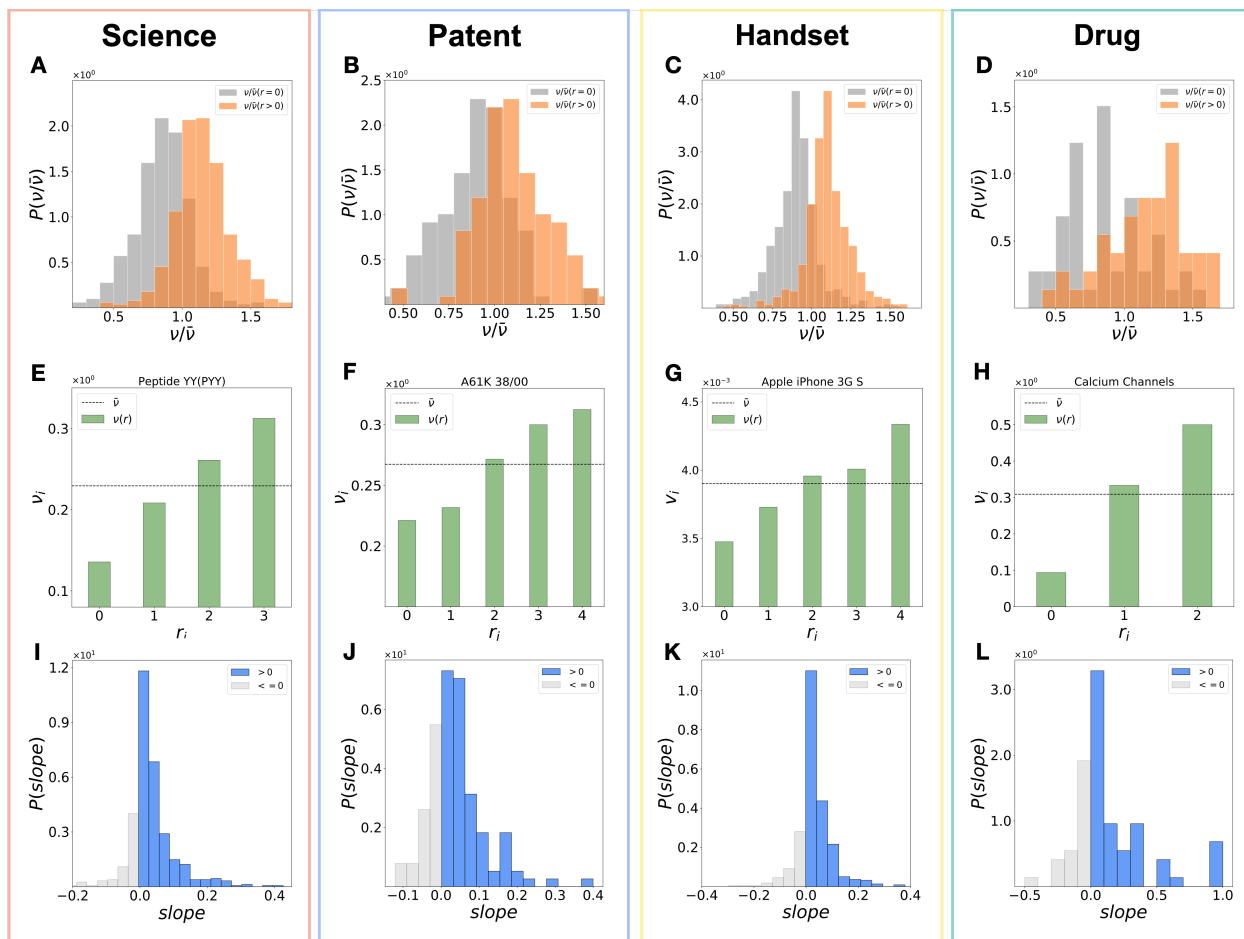


Figure 2: **Innovation abandonment and the underlying social network.** (A-D) Distributions of abandonment probability plotted separately for people whose network neighbors have abandoned the innovation (orange) or not (grey). Here we control for temporal effects by taking a small time interval for our measurements (one year for the scientific fields, patenting domains and drug MOAs, and 100 days for the mobile handsets). To maintain consistency of measurements across the four domains, we begin our measurements around an innovation’s half-life, i.e., when its popularity reduces to half of its peak. We find the two distributions deviate from each other, suggesting that the underlying network further plays a role in abandonment dynamics. (E-H) Abandonment probability  $v_i$  as a function of  $r_i$  for one innovation selected from each domain as an illustrative example (*Peptide YY* for scientific fields, *A61K 38/00* for patenting domains, iPhone 3GS for handsets and *Drugs Targeting Calcium Channels (Voltage-Gated)* for drug MOAs, respectively). Dashed line indicates the null model, where abandonment probability is independent of how many network neighbors have abandoned the innovation ( $r_i$ ). (I-L) We estimate the relationship between the abandonment probability  $v_i$  and  $r_i$  for all scientific fields (I), patenting domains (J), mobile handsets (K) and drug MOAs (L) and plot the distribution of the coefficients, finding a vast majority of them can be approximated by a positive slope.

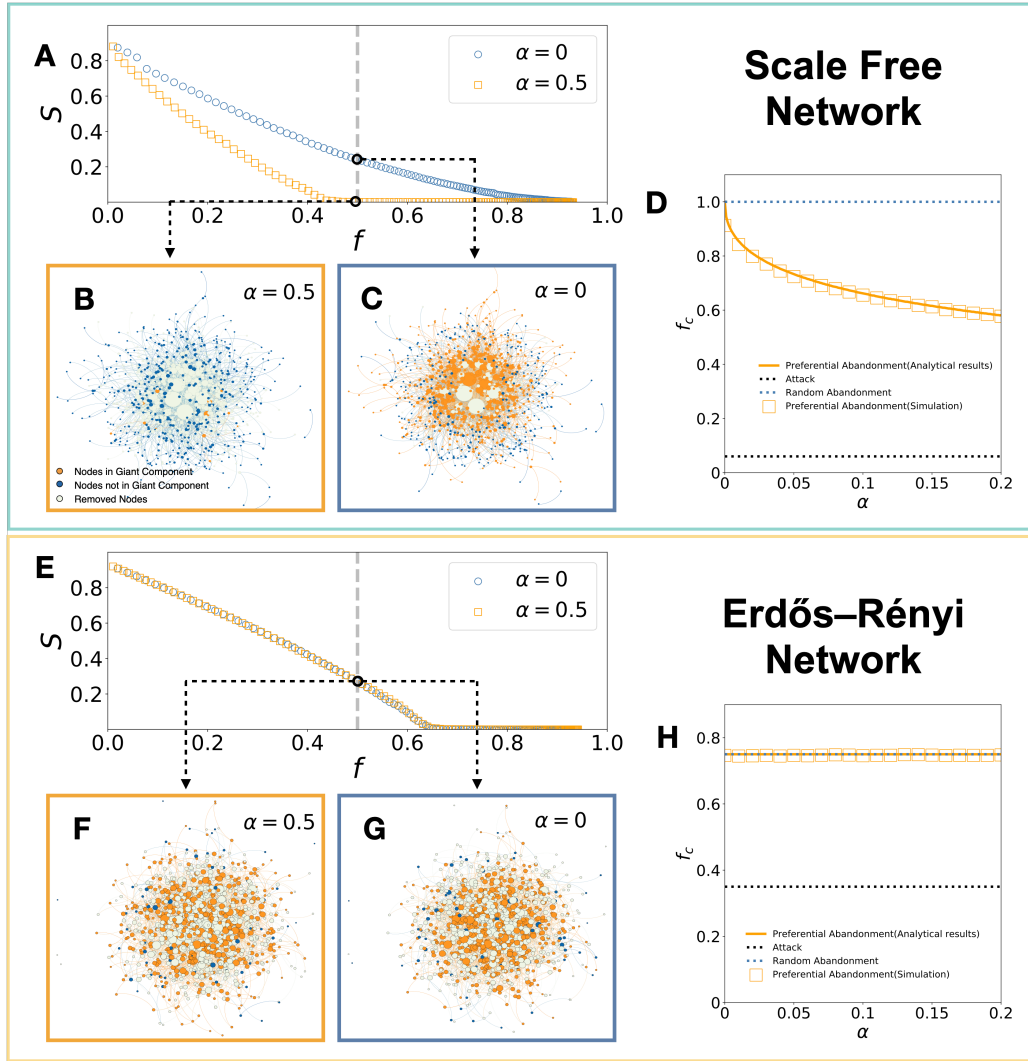
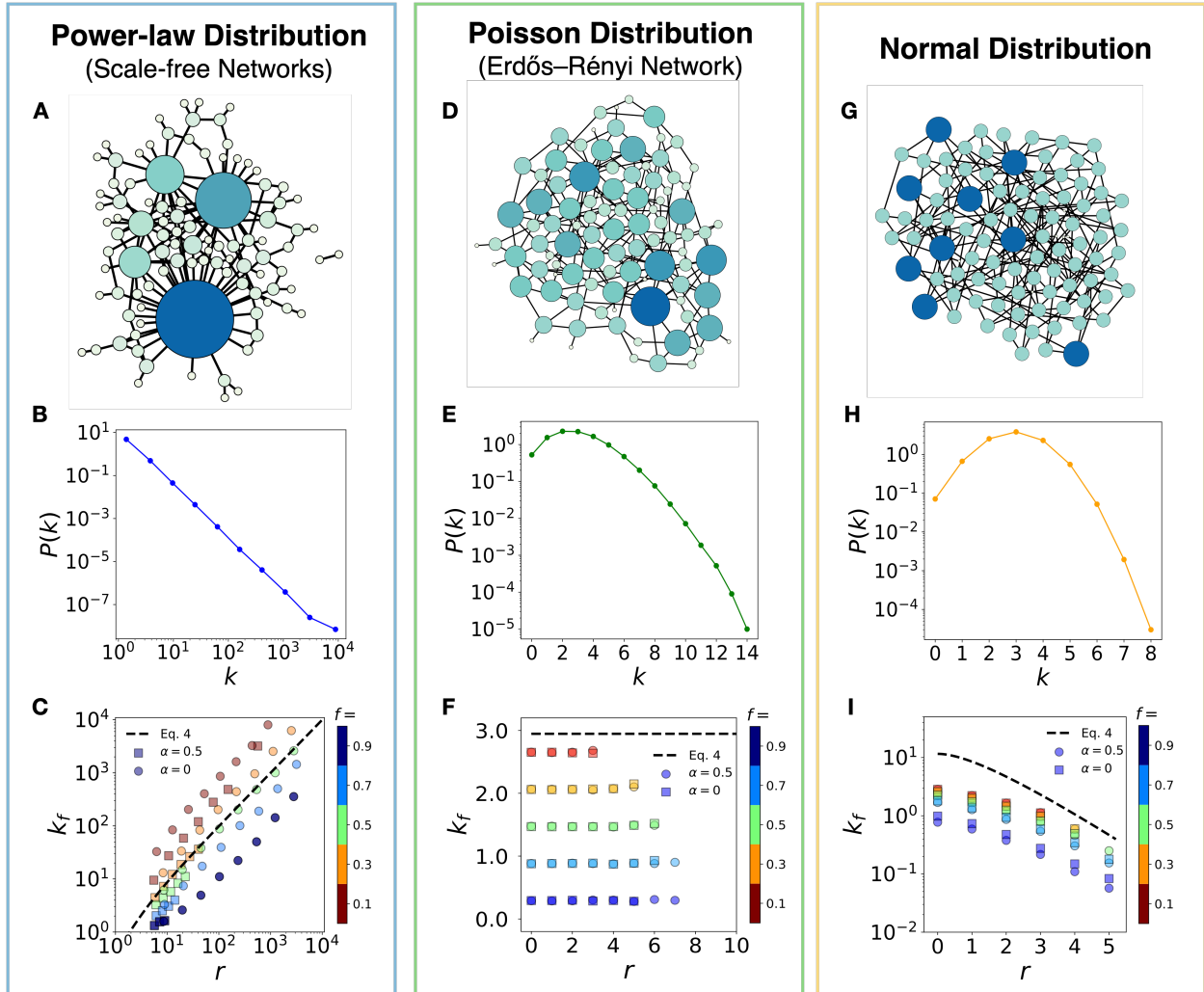


Figure 3: **Preferential abandonment on scale-free network and Erdos-Renyi network.** Simulations of abandonment dynamics on a scale-free network with exponent  $\gamma = 2.5$  (A-D) and an ER network with the same average degree (E-H). The simulations are performed on networks with  $N = 10^6$ , and averaged over 100 realizations. (A, E) show the change of the network's giant component  $S$  as a fraction of nodes ( $f$ ) removed from the system, for preferential abandonment process with  $\alpha = 0.5$  and the random abandonment process where  $\alpha = 0$ . (B, C, F, G) Visualizations of the network when half of its nodes have abandoned the innovation, under preferential abandonment (B, F) and random abandonment (C, G) on a scale-free network (B, C) and an ER network (F, G). Here the nodes that have abandoned the innovation are colored grey, and for the remaining nodes, those in the giant connected component are colored orange; blue otherwise. (D, H) The location of the critical points as a function of  $\alpha$  for scale-free networks (D). We plot the critical points under preferential abandonment on a scale free network with  $\gamma = 2.5$  (orange squares for simulation and orange line for its analytical solution). In comparison, we also plot the results for attacks on a scale free network (black dotted line), and under random abandonment (blue dotted line). We repeat the same analyses for ER networks in (H).



**Fig.4. Theoretical framework of different network topology.** (A) A toy visualization of networks with power-law degree distribution. (B) The degree distribution of the simulated scale-free network with exponent  $\gamma = 2.5$  and  $N = 10^6$ . (C) The relationship between  $k_f$  (current degree) and  $r$  (number of abandoned neighbors) for each time snapshot,  $f = 0.1, 0.3, 0.5, 0.7, 0.9$ , is obtained from Monte Carlo simulation under random abandonment (circles) and preferential abandonment (squares) with  $\alpha = 0.5$  on scale-free networks. The dashed black line refers to Eq. (4), showing the asymptotic trend of  $k_f$  in large  $r$  regime (see SI S4 for details). (D) A toy visualization of ER network. (E) The degree distribution and  $k_f - r$  relationship for a simulated ER network with the same average degree and number of nodes. (G) A toy visualization of networks with normal degree distribution. (H) The degree distribution and  $k_f - r$  relationship for a simulated network with normal degree distribution, controlled for the same average degree and number of nodes.

## Reference

1. Rogers, E.M., *Diffusion of innovations*. 1962: Simon and Schuster.
2. Bernoulli, D., *Essai d'une nouvelle analyse de la mortalité causée par la petite vérole, et des avantages de l'inoculation pour la prévenir*. Histoire de l'Acad., Roy. Sci.(Paris) avec Mem, 1760: p. 1-45.
3. Merton, R.K., *The Matthew effect in science: The reward and communication systems of science are considered*. Science, 1968. **159**(3810): p. 56-63.
4. Price, D.J.D.S., *Networks of scientific papers: The pattern of bibliographic references indicates the nature of the scientific research front*. Science, 1965. **149**(3683): p. 510-515.
5. Evans, J.A. and J.G. Foster, *Metaknowledge*. Science, 2011. **331**(6018): p. 721-725.
6. Fortunato, S., et al., *Science of science*. Science, 2018. **359**(6379): p. eaao0185.
7. Wang, D. and A.-L. Barabási, *The science of science*. 2021: Cambridge University Press.
8. Bass, F.M., *A new product growth for model consumer durables*. Management science, 1969. **15**(5): p. 215-227.
9. Christensen, C.M., *The innovator's dilemma: when new technologies cause great firms to fail*. 2013: Harvard Business Review Press.
10. Mahajan, V., E. Muller, and F.M. Bass, *New product diffusion models in marketing: A review and directions for research*. Journal of marketing, 1990. **54**(1): p. 1-26.
11. Pastor-Satorras, R. and A. Vespignani, *Epidemic spreading in scale-free networks*. Physical review letters, 2001. **86**(14): p. 3200.
12. Colizza, V., et al., *The role of the airline transportation network in the prediction and predictability of global epidemics*. Proceedings of the National Academy of Sciences, 2006. **103**(7): p. 2015-2020.
13. Brockmann, D. and D. Helbing, *The hidden geometry of complex, network-driven contagion phenomena*. science, 2013. **342**(6164): p. 1337-1342.
14. Pastor-Satorras, R., et al., *Epidemic processes in complex networks*. Reviews of modern physics, 2015. **87**(3): p. 925.
15. Granovetter, M., *Threshold models of collective behavior*. American journal of sociology, 1978. **83**(6): p. 1420-1443.
16. Christakis, N.A. and J.H. Fowler, *The spread of obesity in a large social network over 32 years*. New England journal of medicine, 2007. **357**(4): p. 370-379.
17. Banerjee, A., et al., *The diffusion of microfinance*. Science, 2013. **341**(6144).
18. Leskovec, J., L.A. Adamic, and B.A. Huberman, *The dynamics of viral marketing*. ACM Transactions on the Web (TWEB), 2007. **1**(1): p. 5-es.
19. Centola, D. and M. Macy, *Complex contagions and the weakness of long ties*. American journal of Sociology, 2007. **113**(3): p. 702-734.
20. Aral, S., L. Muchnik, and A. Sundararajan, *Distinguishing influence-based contagion from homophily-driven diffusion in dynamic networks*. Proceedings of the National Academy of Sciences, 2009. **106**(51): p. 21544-21549.
21. Lazer, D., et al., *Computational social science*. Science, 2009. **323**(5915): p. 721-723.
22. Macy, M., et al., *Opinion cascades and the unpredictability of partisan polarization*. Science advances, 2019. **5**(8): p. eaax0754.

23. Pentland, A., *Social physics: How good ideas spread-the lessons from a new science*. 2014: Penguin.
24. Vosoughi, S., D. Roy, and S. Aral, *The spread of true and false news online*. *science*, 2018. **359**(6380): p. 1146-1151.
25. Kuhn, T., *The structure of scientific revolutions*. 1996: Princeton University Press.
26. Saavedra, S., F. Reed-Tsochas, and B. Uzzi, *Asymmetric disassembly and robustness in declining networks*. *Proceedings of the National Academy of Sciences*, 2008. **105**(43): p. 16466-16471.
27. Wang, D., C. Song, and A.-L. Barabási, *Quantifying long-term scientific impact*. *Science*, 2013. **342**(6154): p. 127-132.
28. Yin, Y. and D. Wang, *The time dimension of science: Connecting the past to the future*. *Journal of Informetrics*, 2017. **11**(2): p. 608-621.
29. Candia, C., et al., *The universal decay of collective memory and attention*. *Nature human behaviour*, 2019. **3**(1): p. 82-91.
30. Machlup, F., *The production and distribution of knowledge in the United States*. Vol. 278. 1962: Princeton university press.
31. Berger, J. and G. Le Mens, *How adoption speed affects the abandonment of cultural tastes*. *Proceedings of the National Academy of Sciences*, 2009. **106**(20): p. 8146-8150.
32. Arbesman, S., *The half-life of facts: Why everything we know has an expiration date*. 2013: Penguin.
33. Hethcote, H.W., *The mathematics of infectious diseases*. *SIAM review*, 2000. **42**(4): p. 599-653.
34. Scarpino, S.V. and G. Petri, *On the predictability of infectious disease outbreaks*. *Nature communications*, 2019. **10**(1): p. 898.
35. Karsai, M., et al., *Complex contagion process in spreading of online innovation*. *Journal of The Royal Society Interface*, 2014. **11**(101): p. 20140694.
36. Ruan, Z., et al., *Kinetics of social contagion*. *Physical review letters*, 2015. **115**(21): p. 218702.
37. Jin, C., et al., *Emergence of scaling in complex substitutive systems*. *Nature human behaviour*, 2019. **3**(8): p. 837-846.
38. Iacopini, I., et al., *Simplicial models of social contagion*. *Nature communications*, 2019. **10**(1): p. 2485.
39. Hill, A.L., et al., *Infectious disease modeling of social contagion in networks*. *PLOS computational biology*, 2010. **6**(11): p. e1000968.
40. de Arruda, G.F., G. Petri, and Y. Moreno, *Social contagion models on hypergraphs*. *Physical Review Research*, 2020. **2**(2): p. 023032.
41. Katz, M.L. and C. Shapiro, *Network externalities, competition, and compatibility*. *The American economic review*, 1985. **75**(3): p. 424-440.
42. Aral, S. and D. Walker, *Identifying influential and susceptible members of social networks*. *Science*, 2012. **337**(6092): p. 337-341.
43. Rao, H., H.R. Greve, and G.F. Davis, *Fool's gold: Social proof in the initiation and abandonment of coverage by Wall Street analysts*. *Administrative science quarterly*, 2001. **46**(3): p. 502-526.
44. Schilling, M.A., *Technology success and failure in winner-take-all markets: The impact of learning orientation, timing, and network externalities*. *Academy of management journal*, 2002. **45**(2): p. 387-398.

45. Barabási, A.-L. and R. Albert, *Emergence of scaling in random networks*. science, 1999. **286**(5439): p. 509-512.
46. Burns, L.R. and D.R. Wholey, *Adoption and abandonment of matrix management programs: Effects of organizational characteristics and interorganizational networks*. Academy of management journal, 1993. **36**(1): p. 106-138.
47. Greenwood, B.N., et al., *The when and why of abandonment: The role of organizational differences in medical technology life cycles*. Management Science, 2017. **63**(9): p. 2948-2966.
48. Greve, H.R., *Jumping ship: The diffusion of strategy abandonment*. Administrative Science Quarterly, 1995: p. 444-473.
49. Gaba, V. and G. Dokko, *Learning to let go: Social influence, learning, and the abandonment of corporate venture capital practices*. Strategic management journal, 2016. **37**(8): p. 1558-1577.
50. Sinha, A., et al. *An overview of microsoft academic service (mas) and applications*. in *Proceedings of the 24th international conference on world wide web*. 2015.
51. Lou, B. and L. Wu, *AI on Drugs: Can Artificial Intelligence Accelerate Drug Development? Evidence from a Large-scale Examination of Bio-pharma Firms*. MIS Quarterly, 2021. **45**(3).
52. Krieger, J.L., *Trials and terminations: Learning from competitors' R&D failures*. Management Science, 2021. **67**(9): p. 5525-5548.
53. Newman, M.E., *The structure of scientific collaboration networks*. Proceedings of the national academy of sciences, 2001. **98**(2): p. 404-409.
54. Schumpeter, J.A., *Capitalism, Socialism, and Democracy*. 1942.
55. White, H.C., *Chains of opportunity*. 2013: Harvard University Press.
56. Barabási, A.-L., *Network science*. Network Science. 2016: Cambridge University Press.
57. Newman, M., *Networks*. 2018: Oxford university press.
58. Albert, R., H. Jeong, and A.-L. Barabási, *Error and attack tolerance of complex networks*. nature, 2000. **406**(6794): p. 378-382.
59. Cohen, R., et al., *Resilience of the internet to random breakdowns*. Physical review letters, 2000. **85**(21): p. 4626.
60. Cohen, R., et al., *Breakdown of the internet under intentional attack*. Physical review letters, 2001. **86**(16): p. 3682.
61. Callaway, D.S., et al., *Network robustness and fragility: Percolation on random graphs*. Physical review letters, 2000. **85**(25): p. 5468.
62. Li, M., et al., *Percolation on complex networks: Theory and application*. Physics Reports, 2021. **907**: p. 1-68.
63. Allard, A., et al., *Asymmetric percolation drives a double transition in sexual contact networks*. Proceedings of the National Academy of Sciences, 2017. **114**(34): p. 8969-8973.
64. Dodds, P.S. and D.J. Watts, *Universal behavior in a generalized model of contagion*. Physical review letters, 2004. **92**(21): p. 218701.
65. Garcia, D., P. Mavrodiev, and F. Schweitzer. *Social resilience in online communities: The autopsy of friendster*. in *Proceedings of the first ACM conference on Online social networks*. 2013.
66. Török, J. and J. Kertész, *Cascading collapse of online social networks*. Scientific reports, 2017. **7**(1): p. 16743.



67. Yehezkel, A. and R. Cohen, *Degree-based attacks and defense strategies in complex networks*. Physical Review E, 2012. **86**(6): p. 066114.
68. Tian, L., et al., *Articulation points in complex networks*. Nature communications, 2017. **8**(1): p. 1-9.
69. Motter, A.E. and Y.-C. Lai, *Cascade-based attacks on complex networks*. Physical Review E, 2002. **66**(6): p. 065102.
70. Goh, K.-I., et al., *Sandpile on scale-free networks*. Physical review letters, 2003. **91**(14): p. 148701.
71. Dobson, I., et al., *Complex systems analysis of series of blackouts: Cascading failure, critical points, and self-organization*. Chaos: An Interdisciplinary Journal of Nonlinear Science, 2007. **17**(2): p. 026103.

# Supplementary Information for Quantifying the Dynamics of Innovation Abandonment Across Scientific, Technological, Commercial, and Phar- macological Domains

Binglu Wang<sup>1,2,3\*</sup>, Ching Jin<sup>1,2,3,4\*</sup>, Chaoming Song<sup>5</sup>, Johannes Bjelland<sup>6</sup>, Brian Uzzi<sup>1,2,3</sup> & Dashun Wang<sup>1,2,3†</sup>

<sup>1</sup>*Center for Science of Science and Innovation, 600 Foster Street, Evanston, IL 60208, USA*

<sup>2</sup>*Northwestern Institute on Complex Systems (NICO), 600 Foster Street, Evanston, IL 60208, USA*

<sup>3</sup>*Kellogg School of Management, 2211 Campus Dr, Evanston, IL 60208, USA*

<sup>4</sup>*Centre for Interdisciplinary Methodologies, University of Warwick, Coventry, CV4 7AL, United Kingdom*

<sup>5</sup>*Department of Physics, University of Miami, 1320 S Dixie Hwy, Coral Gables, FL 33146, USA*

<sup>6</sup>*Telenor Research and Development, Snarøyveien 30 N-1360 Fornebu, Norway*

*\*These authors contributed equally to this work.*

*†Correspondence should be addressed to D.W. (dashun.wang@kellogg.northwestern.edu)*

# Contents

<b>S1 Dataset Descriptions</b>	<b>4</b>
S1.1 $D_1$ : Abandonment of Scientific Fields . . . . .	4
S1.2 $D_2$ : Abandonment in Patenting . . . . .	5
S1.3 $D_3$ : Abandonment of Mobile Handsets . . . . .	5
S1.4 $D_4$ : Abandonment in Pharmacological Innovation . . . . .	6
<b>S2 Empirical Methods</b>	<b>7</b>
S2.1 Degree Distribution of Different Social Systems . . . . .	7
S2.2 Selecting Time Intervals to Measure the Structural Effect . . . . .	7
S2.3 Robustness Check on Different Time Intervals . . . . .	8
<b>S3 Heterogenous Mean-Field Theory</b>	<b>9</b>
S3.1 Method Description . . . . .	9
S3.2 Express $i_k$ as a Function of $t$ . . . . .	10
S3.3 Relationship between $i'_k$ and $i_k$ . . . . .	11
S3.4 Express $i_k$ as a Function of $f$ . . . . .	12
S3.5 Molloy-Reed Criterion Method . . . . .	13
<b>S4 Relationship between <math>k_f</math> and <math>r</math></b>	<b>14</b>
S4.1 Relationship between $k_f$ and $r$ in Different Network Structures . . . . .	14
S4.2 $k_f$ as a Function of $r$ . . . . .	18
1. Random Abandonment ( $\alpha = 0$ ) . . . . .	18

2.  $\alpha > 0$  (Preferential Abandonment) . . . . . 23

**S5 Supplementary References** . . . . . **30**

**30**

# S1 Dataset Descriptions

## S1.1 $D_1$ : Abandonment of Scientific Fields

The first dataset ( $D_1$ ) tracks the dynamics of research fields through the publication records of individual scientists (172 million papers indexed by the Microsoft Academic Graph<sup>1</sup>), using the field classification provided by MAG<sup>2</sup>.

*Identifying Abandonment of Scientific Fields for Each Scientist:* MAG’s field classification follows a hierarchical structure. We focus on leaf fields (i.e., fields without child fields), except when a field has fewer than 500 publications or more than three levels of parent fields, in which case we trace their corresponding parent fields instead. To estimate when a scholar abandons a field, we consider the year when the scholar’s primary research focus shifts away from a field after having spent at least two years in it. Fig. S1 illustrates this process. Specifically, we follow three steps: (1) list all publications of the scholar associated with at least one leaf field; (2) identify the field in which the scholar published the most papers each year as their primary research focus; and (3) construct the scholar’s career history based on their annual research focus. These steps allow us to determine when a scientist no longer focuses on a specific scientific field. Our analysis includes scientists (1) whose publishing career spans at least 10 years and (2) who have published at least 10 papers.

In total,  $D_1$  records 990K scientists studying 1,219 fields that emerged after 1940 and were

studied by at least 500 scientists from 1940 to 2015.

## **S1.2 $D_2$ : Abandonment in Patenting**

The second dataset ( $D_2$ ) captures 6.9 million patents granted by the USPTO from 1976 to 2015. To approximate patenting domains, we focus on the abandonment dynamics of each subgroup in the CPC codes.

*Identifying Abandonment of Patenting Domains for Each Inventor:* Similar to  $D_1$ , we construct the career history of each inventor by identifying their patenting focus each year, defined as the subgroup with the most patents. Based on the annual domain focus of each inventor, we determine the abandonment of patenting domains when they stop focusing their patenting activities on certain domains.

We focus on patenting domains that involved at least 200 inventors from 1976 to 2015. In total,  $D_2$  records 123K inventors with more than five years of patenting careers across 291 domains from 1976 to 2015.

## **S1.3 $D_3$ : Abandonment of Mobile Handsets**

The third dataset ( $D_3$ ) captures the commercial domain of mobile handsets, recording individual usage history provided by a European telecommunication company. We identify the abandonment

of mobile handsets by tracking changes in their daily active users from 2006 to 2014.

*Identifying Abandonment of Mobile Handsets for Each Consumer:* We determine the abandonment of mobile handsets by each user through SIM card records, which provide clear timelines for when users change mobile phones. Specifically, we use the last usage day of a mobile handset as the user's abandonment time for that handset.

We focus on mobile handsets used by more than 1,000 users. In total,  $D_3$  records 3.5M users using 704 types of mobile handsets from 2006 to 2014.

#### **S1.4 $D_4$ : Abandonment in Pharmacological Innovation**

The fourth dataset ( $D_4$ ) traces the dynamics of pharmacological innovations using the Cortellis Drug Discovery Intelligence database, which contains the largest and most detailed drug development records globally, covering 648,702 drugs over the past 25 years.

*Identifying Abandonment of MOAs for Each Pharmaceutical Organization:* To quantify the abandonment dynamics of pharmacological innovations, we examine biological mechanisms of action (MOAs) associated with each drug and measure the market focus of pharmaceutical companies on these MOAs. Abandonment is defined as the year when pharmaceutical organizations cease adopting specific MOAs in clinical trials.

We focus on second-level and higher MOAs adopted by at least 10 organizations. In total,  $D_4$

tracks 248 MOAs used by 5,133 pharmaceutical companies, measuring the fraction of companies using each MOA in drug development.

## **S2 Empirical Methods**

### **S2.1 Degree Distribution of Different Social Systems**

The present study investigates the decline of robust network systems, which are the predominant network type in the social world<sup>3</sup>. To this end, we first plotted the degree distribution of the four systems (i.e., science dataset, patent dataset, handset dataset, and drug dataset) in Fig. S2. Our findings indicate that the degree distributions exhibit a fat-tail in all four datasets.

### **S2.2 Selecting Time Intervals to Measure the Structural Effect**

In Fig. 2, we measure the structural effect within a small time interval to control for temporal effects. To maintain consistency of measurements across the four domains, we focus on the time when an innovation reaches its half-life, i.e., when the popularity has been reduced to half of its peak. For  $D_1$ ,  $D_2$ , and  $D_4$ , we measure the structural effect on a minimal time scale—one year after the half-life. For  $D_3$ , we observe the abandonments within 100 days around the half-life, since the dataset provides daily activities.



## S2.3 Robustness Check on Different Time Intervals

To check the robustness of the observed structural effect, we repeat the analyses of Fig. 2 in the main text for different time intervals. Specifically, we test the structural effect when the popularity has been reduced to 60% (Fig. S3) and 40% (Fig. S4) of the maximum in addition to the half-life (50%, in the main text), finding the observed phenomenon is robust.

In both Fig. S3 and Fig. S4, we separate the individuals and organizations in our datasets into two groups, based on whether or not abandonments have occurred among their network neighbors ( $r_i > 0$  vs.  $r_i = 0$ ), and measure the rate of abandonment separately for the two groups. We find that the distributions of abandonment rate for the two groups show visibly different patterns (ABCD in both figures), with the distribution for the first group ( $r_i > 0$ ) shifting systematically to the right of the  $r_i = 0$  group. This suggests that the abandonment rate is higher when abandonments have occurred within the network neighbors. To systematically test across different innovations in different domains, we fit the relationship between  $\nu_i$  and  $r_i$  for each scientific field, patenting domain, mobile handset, and drug MOAs, respectively, with a linear model, finding that a substantial fraction of scientific, technological, commercial, and pharmacological innovations can be approximated by a positive slope (72.84%, 72.73%, 79.28% and 64.37%, respectively in Fig. S3 EFGH; 70.78%, 57.41%, 78.38% and 60.38%, respectively in Fig. S4 EFGH).

## S3 Heterogenous Mean-Field Theory

### S3.1 Method Description

To better understand the phase transition phenomenon in the small  $\alpha$  region, we adopt the heterogeneous mean-field approximation (HMA)—a frequently used analytical method in epidemiology, network science, and percolation theory<sup>4,5</sup>. HMA assumes that nodes with the same degree follow the same behavior. By denoting  $i_k$  as the survival probability of a node with degree  $k$ , we can express the fraction of abandoned nodes  $f$  in the system as:

$$f = 1 - \sum_k P_k i_k, \quad (\text{S1})$$

where  $P_k$  is the degree distribution.

To identify the critical point  $f_c$  at which the giant component vanishes, we calculate  $u$ , the probability that a remaining node does not belong to the giant component.  $u$  is a function of  $f$  satisfying the following equation<sup>5</sup>:

$$u = \sum_k q_k (1 - i'_{k+1} + i'_{k+1} u^k), \quad (\text{S2})$$

where  $q_k$  corresponds to the excess degree distribution of the network, and  $i'_{k+1}$  is the *neighbor-weighted survival probability* for nodes with degree  $k+1$ . This probability quantifies the likelihood that a node with degree  $k+1$  survives when we first randomly select a surviving node and then randomly pick one of its neighbors with degree  $k+1$ . Notice that  $i'_{k+1}$  is different to  $i_{k+1}$ .  $i_{k+1}$  is a *direct survival probability*—it directly counts how many nodes with degree  $k+1$  survive, without

considering how these nodes are connected to others.  $i'_{k+1}$  is more complex- here, we consider the process of reaching nodes through their neighbors, which introduces a bias: nodes with more connections (i.e., higher-degree nodes) are more likely to be picked multiple times since they have more neighbors. We will present the quantitative relationship between  $i_{k+1}$  and  $i'_{k+1}$  in later sections.

Equation (S2) suggests that if a node is not connected to the giant component, it either links to a node who is also not in the giant component or the node has already been removed. Based on percolation theory, the giant component vanishes when the derivative of the right-hand side equals 1 at  $u = 1$ . In other words:

$$\left[ \frac{d}{du} \sum_k q_k (1 - i'_{k+1} + i'_{k+1} u^k) \right]_{u=1} = 1. \quad (\text{S3})$$

The phase transition point  $f_c$  can be obtained through equation (S3). To achieve this, we need to express  $i_k$  in terms of  $f$  and substitute it back into equation (S3).

### S3.2 Express $i_k$ as a Function of $t$ .

Let us first express  $i_k$  in terms of  $t$ , we have:

$$\frac{di_k}{dt} = -i_k \nu_0 [\alpha k \mu(t) + (1 - \alpha)]. \quad (\text{S4})$$

Here,  $\mu(t) \equiv 1 - \sum_{k'} q_{k'} (i'_{k'+1})$  measures the probability that a remaining node is linked to a neighbor who has abandoned the product. Solving for (S4), we have:

$$i_k = e^{-\nu_0(1-\alpha)t} [h(t)]^k, \quad (\text{S5})$$

where  $h$  is a function satisfying:

$$\frac{dh}{dt} = -\nu_0\alpha\mu h. \quad (\text{S6})$$

By inserting (S5) into the definition of  $\mu$ , we can express  $\mu$  as a function of  $h$ :

$$\mu(t) = 1 - e^{-\nu_0(1-\alpha)t}G_1(h)/h, \quad (\text{S7})$$

where  $G_1(x) \equiv \sum_k \frac{1}{\langle k \rangle} (k+1)P(k+1)x^k$  is the generating function for excess degree. Here we have also used an important relation:  $i'_k/i_k = 1/h^2$ , which will be proved in S3.3. Combing (S7) and (S6), we have:

$$\frac{dh}{dt} = -\nu_0\alpha(h - e^{-\nu_0(1-\alpha)t}G_1(h)). \quad (\text{S8})$$

### S3.3 Relationship between $i'_k$ and $i_k$ .

Since  $i'_k$  measures the surviving probability of  $k$ -degree nodes through the nodes' surviving neighbors, nodes with more surviving neighbors will contribute more to the probability. We have:

$$\begin{aligned} \frac{di'_k}{dt} &= -i'_k\nu_0\left[(1-\alpha) + \alpha \frac{\sum_{m=0}^{k-1} (k-1-m)m(1-\mu)^m\mu^{k-m-1}}{\sum_{m=0}^{k-1} m(1-\mu)^m\mu^{k-m-1}}\right] \\ &= -i'_k\nu_0\left[(1-\alpha) + \alpha \frac{(k-1)^2(1-\mu) - (k-1)(1-\mu)\mu - (k-1)^2(1-\mu)^2}{(k-1)(1-\mu)}\right] \quad (\text{S9}) \\ &= -i'_k\nu_0[(1-\alpha) + \alpha(k-2)\mu], \end{aligned}$$

where  $m$  measures the number of removed neighbors of the studied node. The reason the sum runs from 0 to  $k-1$  instead of to  $k$  is because the node is reached through a surviving node, therefore, the maximum number of removed neighbor is  $k-1$ . Solving this equation, it is easy to obtain:

$$i'_k = e^{-\nu_0(1-\alpha)t}[h(t)]^{k-2}. \quad (\text{S10})$$

Combining S10 and S5, we have:

$$i'_k/i_k = \frac{1}{h^2} \quad (\text{S11})$$

### S3.4 Express $i_k$ as a Function of $f$ .

Combing Eq. S5 and Eq. S1, we have:

$$e^{-\nu_0(1-\alpha)t} = \frac{1-f}{G_0(h)}. \quad (\text{S12})$$

By inserting it back to Eq. S5 and Eq. S8, we have:

$$i_k = \frac{1-f}{G_0(h)} h^k, \quad (\text{S13})$$

and

$$\frac{dh}{df} = \frac{-\alpha h G_0^2(h) + \alpha G_0(h) G_1(h) (1-f)}{\alpha(1-f) h G_0(h) G_0'(h) - \alpha(1-f)^2 G_0'(h) G_1(h) + (1-\alpha)(1-f) G_0^2(h)}, \quad (\text{S14})$$

where  $G_0$  and  $G_1$  are generating functions, defined as  $G_0(x) \equiv \sum_k P(k)x^k$ ,  $G_1(x) \equiv \sum_k \frac{1}{\langle k \rangle} (k+1)P(k+1)x^k$ . Inserting (S13) to (S3), we may obtain the self-consistent equation for  $f_c$ :

$$f_c = 1 - \frac{G_0(h_c) \langle k \rangle}{G_0''(h_c)} = 1 - \frac{\langle k \rangle \sum_k P_k h_c^k}{\sum_k P_k (k^2 - k) h_c^{k-2}}, \quad (\text{S15})$$

where  $h_c$  is the solution of Eq. S14 for  $f = f_c$ .

### S3.5 Molloy-Reed Criterion Method

An alternative method for identifying the phase transition point is through the Molloy-Reed Criterion<sup>3,6</sup>: a network with any degree distribution has a giant component if

$$\frac{\langle k^2 \rangle}{\langle k \rangle} > 2. \quad (\text{S16})$$

We first calculate for the average degree of a network when  $f$  fraction of nodes have been removed:

$$\begin{aligned} \langle k' \rangle_f &= \frac{\sum P_k i_k \binom{k}{k'} k' \mu^{k-k'} (1-\mu)^{k'}}{\sum P_k i_k} \\ &= \frac{\sum_k k h^k P_k (1-\mu)}{G_0(h)} \\ &= \frac{(1-\mu) G'_0(h) h}{G_0(h)} \\ &= \frac{(1-f) G'_0(h) G_1(h)}{G_0^2(h)}. \end{aligned} \quad (\text{S17})$$

In the same way, we can calculate  $\langle k'^2 - k' \rangle$ :

$$\begin{aligned} \langle k'^2 - k' \rangle_f &= \frac{\sum P_k i_k \binom{k}{k'} (k'^2 - k') \mu^{k-k'} (1-\mu)^{k'}}{\sum P_k i_k} \\ &= \frac{\sum_k (k^2 - k) h^k P_k (1-\mu)^2}{G_0(h)} \\ &= (1-f)^2 \frac{G''_0(h) G_1^2(h)}{G_0^3(h)}. \end{aligned} \quad (\text{S18})$$

By combining these results we have:

$$f_c = 1 - \frac{G_0(h_c) \langle k \rangle}{G''_0(h_c)} = 1 - \frac{\langle k \rangle \sum_k P_k h_c^k}{\sum_k P_k (k^2 - k) h_c^{k-2}}, \quad (\text{S19})$$

which is consistent with our previous findings.

## S4 Relationship between $k_f$ and $r$

### S4.1 Relationship between $k_f$ and $r$ in Different Network Structures

Why is the relationship between  $k_f$  and  $r$  different across various networks? An intuitive understanding can be gained by analyzing the initial step of the process, where the first fraction  $f_0$  of nodes are removed from a generated network. The process is a simple Poisson process, where the joint probability of the current degree  $k$  and  $r$  can be written as:  $P_{f_0}(k, r) = P(k+r) \binom{k+r}{r} (1-f)^k f^r$ . For an ER network, the formation process is also a Poisson process, where each node is independently connected to other nodes with the same probability. Since each node behaves independently in both the formation and removal processes, the distributions of  $k$  and  $r$  should also be independent. Mathematically, we have:

$$P_{f_0}(k, r) = \frac{\lambda^{k+r} e^{-\lambda}}{(k+r)!} \binom{k+r}{r} (1-f)^k f^r = \frac{[\lambda(1-f)]^k e^{-\lambda(1-f)}}{k!} \frac{[\lambda(1-f)]^r e^{-\lambda(1-f)}}{r!} \quad (\text{S20})$$

Here,  $P_{f_0}(k, r)$  can be decoupled into two independent distributions for  $k$  and  $r$ , suggesting that the process can be viewed as two independent processes. In the next section, we show that not only in the initial step but in all steps of the ER network, the joint probability can be decoupled, demonstrating the independence of the current degree  $k$  and  $r$ . The key to this decoupling property is the factorial decay of the Poisson process, which must satisfy two criteria: 1) each node is independently attached to other nodes (Independence), and 2) each node attaches to other nodes with the same probability (Homogeneity).

For a network with heavy tails, the formation process can be represented as an inhomogeneous Poisson process (see hidden variable network models), where each node attaches to others independently but with a different probability. A node with a higher probability is more likely to have a higher  $r$  and a higher current degree, presenting a positive correlation between  $k$  and  $r$ . In contrast, for a network with narrower tails, nodes do not link to others independently, and the degree for each node is bounded. Therefore, removing more neighbors reduces the current degree.

To further understand the process, we also directly study the relationship between  $k_f - r$  for different  $f$  (Fig. S5C). Interestingly, we find that the curves are parallel to each other when  $r$  is relatively large, suggesting that the  $k_f - r$  curve is determined only by the network topology in that condition, and it is irrelevant to the specific dynamics. To test this hypothesis, and to systematically uncover the role of network topology in the abandonment process, we quantify the relationship between  $k_f$  and  $r$  for networks with different degree heterogeneity. We find that although the relationship between  $k_f$  and  $r$  is complex (see the next section for the full mathematical derivation), the asymptotic behavior of  $k_f(r)$  is very simple:

$$k_f(r) \Big|_{r \rightarrow \infty} = W(h)H(r) \sim H(r) \quad (\text{S21})$$

It can be decoupled into two independent factors,  $H(r) \equiv \frac{P_k(r+1)}{P_k(r)}(r+1)$ , and  $P_k(x)$  takes the form of the degree distribution of the network.  $H$  quantifies how fat the degree distribution is compared to a Poisson distribution, and

$$W(h) = \begin{cases} \frac{(1-f)G_1(h)}{G_0(h)-(1-f)G_1(h)} & \text{if } H(r) \Big|_{r \rightarrow \infty} \rightarrow \infty, \\ (1-f)G_1(h)/G_0(h) & \text{if } H(r) \Big|_{r \rightarrow \infty} = H_0, \end{cases} \quad (\text{S22})$$



Since  $W(h)$  is a function independent of  $r$ , Equation (S21) suggests that the trend of  $k_f(r)$  is merely determined by  $H$ , which depends only on the degree distribution of the network.

For ER networks, since the degree distribution follows a Poisson distribution (Fig. S5E), we can calculate that  $\frac{P_k(x+1)}{P_k(x)} = \frac{\lambda}{x+1}$ , and  $H(x) = \lambda$ , suggesting that  $k_f(r)$  remains constant when  $r$  is large (Fig. 4F in the main text). Therefore, under preferential abandonment, where nodes with higher  $r$  are more likely to be abandoned, we effectively select nodes with a random degree  $k_f$ , supporting the conclusion that preferential abandonment is identical to random abandonment on ER networks. Importantly, for ER networks,  $k_f(r)$  remains constant not only for large  $r$  but for any given  $r$ . This result corroborates our findings in Fig. S5F, explaining why the phase transition point does not change in an ER network. It also echoes the analytical results demonstrated in Equation (2) of the main text. The generating functions for ER random networks take special forms:  $G_0(x) = G_1(x) = e^{\langle k \rangle x}$ . By substituting this back into Equation (2) of the main text, we recover the Molloy-Reed criterion:

$$f_c = 1 - \frac{\langle k \rangle}{\langle k^2 \rangle - \langle k \rangle},$$

which is independent of  $\alpha$  (Fig. 3H in the main text, solid line). This result validates that preferential abandonment is exactly the same dynamic process as random abandonment on ER networks.

Empirical networks typically exhibit heavy-tailed degree distributions. From Equation (4), we find that if the degree distribution has a heavier tail than the Poisson distribution, such as a power-law distribution (Fig. S5B),  $H(x)$  grows faster than a constant, indicating a positive correlation between  $k_f$  and  $r$  (Fig. 4C in the main text). Therefore, for these networks, if nodes are

removed under the preferential abandonment process, hubs are more likely to be removed, leading to an earlier phase transition (Fig. S5C). This result supports the argument that preferential abandonment behaves similarly to network attacks (red triangles in Fig. S5C) on heavy-tailed networks. As for networks with narrow degree distributions (i.e., narrower than Poisson), such as networks with a normal degree distribution (Fig. S5H),  $H(x)$  decreases with  $x$ , suggesting a negative correlation between  $k_f$  and  $r$  (Fig. 4I in the main text). Interestingly, the negative relationship between  $k_f$  and  $r$  indicates that if we remove nodes with higher  $r$  under preferential abandonment, we are actually targeting nodes with lower remained degrees, thus inducing a delayed percolation compared to random abandonment (Fig. S5I).

The table below summarizes the prediction for several common networks:

Table 1: Summary of different network structures

Network	Degree Distribution	$H(r)$	$H(r) (r \rightarrow \infty)$
Scale-free networks	$A(\lambda)k^{-\lambda}$	$(r+1)(1+1/r)^{-\lambda}$	$r$
ER networks	$\frac{\lambda^k e^{-\lambda}}{k!}$	$\lambda$	$\lambda$
Gaussian networks	$A(\mu, \sigma)e^{-\frac{1}{2}\left(\frac{k-\mu}{\sigma}\right)^2}$	$(r+1)e^{-\frac{-2r+2\mu-1}{2\sigma^2}}$	$0$

Note:  $A(\lambda)$  and  $A(\mu, \sigma)$  are normalization constants.

## S4.2 $k_f$ as a Function of $r$

In this section, we discuss the average remaining degree of a node after removing a fraction  $f$  of nodes, denoted by  $k_f$ , as a function of the number of removed nodes  $r$ . We begin our analysis with the random abandonment process ( $\alpha = 0$ ) and then proceed to understand the behavior under preferential abandonment.

### 1. Random Abandonment ( $\alpha = 0$ )

For random abandonment, we have the following expression:

$$\begin{aligned} k_f(r) &= \frac{\sum_{k'=0}^{\infty} k' p(k' + r) \binom{k'+r}{k'} f^r (1-f)^{k'}}{\sum_{k'=0}^{\infty} p(k' + r) \binom{k'+r}{k'} f^r (1-f)^{k'}} \\ &= \frac{G_r^{(r+1)}(1-f)}{G_r^{(r)}(1-f)} (1-f), \end{aligned} \quad (\text{S23})$$

where  $G_r(x) = \sum_{k=0}^{\infty} p(k+r)x^{k+r}$ ,  $p(k)$  denotes the degree distribution of the network, and  $G_r^{(n)}(x)$  represents the  $n^{\text{th}}$  derivative of  $G_r(x)$ , i.e.,  $G_r^{(n)}(x) = \frac{\partial^n G_r(x)}{\partial x^n}$ .

Although  $G_r(x)$  is intricate and topology-dependent, its asymptotic behavior can be readily determined. In the limit  $r \rightarrow \infty$ , we have:

$$G_r^{(r)}(x) = \sum_{a=0}^{\infty} (r+a)! p(r+a) \frac{x^a}{a!}. \quad (\text{S24})$$

Additionally, we can write:

$$\begin{aligned}
G_r^{(r+1)}(x) &= \sum_{a=0}^{\infty} \frac{(r+a)! a}{a!} p(r+a) x^{a-1} \\
&= \sum_{a=0}^{\infty} \frac{(r+a+1)!}{a!} p(r+a+1) x^a.
\end{aligned} \tag{S25}$$

Now, by combining equations S24 and S25, we obtain:

$$\begin{aligned}
(1-x)G_r^{(r+1)}(x) &= \sum_{a=0}^{\infty} \left[ \frac{(r+a+1)! p(r+a+1)}{a!} - \frac{(r+a)! a p(r+a)}{a!} \right] x^a \\
\Rightarrow \frac{(1-x)G_r^{(r+1)}(x)}{G_r^{(r)}(x)} &= \frac{\sum_{a=0}^{\infty} \left[ (r+a)! p(r+a) \frac{x^a}{a!} \right] \left[ \frac{(r+a+1)! p(r+a+1)}{(r+a)! p(r+a)} - a \right]}{\sum_{a=0}^{\infty} (r+a)! p(r+a) \frac{x^a}{a!}}.
\end{aligned} \tag{S26}$$

Let us define  $H(r) \equiv (r+1) \frac{p(r+1)}{p(r)}$ . Thus, we have:

$$k_f(r) = \frac{1-f}{f} \frac{\sum_{a=0}^{\infty} \left[ (r+a)! p(r+a) \frac{(1-f)^a}{a!} \right] [H(r+a) - a]}{\sum_{a=0}^{\infty} (r+a)! p(r+a) \frac{(1-f)^a}{a!}}. \tag{S27}$$

Next, we consider the asymptotic properties of  $k_f(r)$  for networks with varying forms of  $H(r)$ .

**Class 1:**  $H(r)|_{r \rightarrow \infty} \rightarrow \infty$

For a network's degree distribution satisfying this condition,  $H(r+a) - a \approx H(r)$  as  $r \rightarrow \infty$ .

Substituting this into Eq. S27, we obtain:

$$k_f(r)|_{r \rightarrow \infty} = \frac{1-f}{f} H(r). \tag{S28}$$

### Example Class 1: Scale-Free Network

A common example of this class is the scale-free network with a power-law degree distribution:

$$\begin{aligned}
p(r) \sim r^{-\beta} \quad \Rightarrow \quad H(r)|_{r \rightarrow \infty} &= (r+1) \left(1 + \frac{1}{r}\right)^{-\beta} \approx (r+1) \left(1 - \frac{\beta}{r}\right) \\
&= r - \beta + 1 - \frac{\beta}{r} = r + O(r) \rightarrow \infty.
\end{aligned} \tag{S29}$$

Thus, for a scale-free network, we have:

$$k_f(r)|_{r \rightarrow \infty} = \frac{1-f}{f} H(r)|_{r \rightarrow \infty} = \frac{1-f}{f} r. \tag{S30}$$

**Class 2:**  $H(r)|_{r \rightarrow \infty} = H_0$  ( $H_0 > 0$ )

For networks with a degree distribution satisfying this condition, we can directly derive:

$$\begin{aligned}
k_f(r)|_{r \rightarrow \infty} &= \frac{1-f}{f} \frac{\sum_{a=0}^{\infty} \left[ (r+a)! p(r+a) \frac{(1-f)^a}{a!} \right] [H(r+a) - a]}{\sum_{a=0}^{\infty} (r+a)! p(r+a) \frac{(1-f)^a}{a!}} \\
&= \frac{1-f}{f} \left( H_0 - \frac{\sum_{a=0}^{\infty} (r+a)! p(r+a) \frac{(1-f)^a}{a!} (a)}{\sum_{a=0}^{\infty} (r+a)! p(r+a) \frac{(1-f)^a}{a!}} \right) \\
&= \frac{1-f}{f} \left( H_0 - \frac{\sum_{a=0}^{\infty} H_0^{r+a} \frac{(1-f)^a}{a!} (a)}{\sum_{a=0}^{\infty} H_0^{r+a} \frac{(1-f)^a}{a!}} \right) \\
&= \frac{1-f}{f} \left( H_0 - \frac{\sum_{a=0}^{\infty} H_0^{r+a} \frac{(1-f)^a}{a!} a}{\sum_{a=0}^{\infty} H_0^{r+a} \frac{(1-f)^a}{a!}} \right) \\
&= \frac{1-f}{f} \left( H_0 - \frac{\sum_{a=0}^{\infty} H_0^a \frac{(1-f)^a}{a!} a}{\sum_{a=0}^{\infty} H_0^a \frac{(1-f)^a}{a!}} \right) \\
&= \frac{1-f}{f} \left( H_0 - \frac{e^{H_0(1-f)} H_0 (1-f)}{e^{H_0(1-f)}} \right) \\
&= (1-f) H_0 = (1-f) H(r)
\end{aligned} \tag{S31}$$

**Example Class 2: Erdős–Rényi (ER) Network**

For the Erdős–Rényi (ER) network, where the degree distribution follows a Poisson distribution,  $H(r)$  is constant:

$$p(r) \sim \frac{e^{-c}c^r}{r!} \quad \Rightarrow \quad H(r) = (r+1)\frac{c}{r+1} = H_0 = c. \quad (\text{S32})$$

Since  $H(r)$  remains constant for all  $r$ , we can calculate  $G_r(x)$  for any  $r$ :

$$\begin{aligned} G_r(x) &= \sum_{k=0}^{\infty} P_k(k+r)x^{k+r} \\ &\sim \sum_{k=0}^{\infty} \frac{e^{-c}c^{k+r}}{(k+r)!} x^{k+r} \\ &= e^{-c} \left( e^{cx} - \sum_{n=0}^{r-1} \frac{(cx)^n}{n!} \right). \end{aligned} \quad (\text{S33})$$

Taking the  $r^{\text{th}}$  and  $(r+1)^{\text{th}}$  derivatives of the second term results in its vanishing. Therefore, we have:

$$k_f(r) = c(1-f) = (1-f)H_0, \quad (\text{S34})$$

which is consistent with Eq. S31.

**Class 3:**  $H(r)|_{r \rightarrow \infty} = 0$

For networks satisfying this condition, we revisit the definitions of  $G_r^{(r)}$  and  $G_r^{(r+1)}$ . For

$$G_r^{(r)}(x) = \sum_{a=0}^{\infty} (r+a)! p(r+a) \frac{x^a}{a!}, \quad (\text{S35})$$

we analyze the ratio of consecutive terms, yielding:

$$\frac{(r+a+1)! p(r+a+1) \frac{x^{a+1}}{(a+1)!}}{(r+a)! p(r+a) \frac{x^a}{a!}} \Big|_{r \rightarrow \infty} = \frac{x}{1+a} H(r) \Big|_{r \rightarrow \infty} = 0. \quad (\text{S36})$$

Thus, only the first term dominates. The same applies to  $G_r^{(r+1)}$ , leading to:

$$G_r^{(r)}(x)|_{r \rightarrow \infty} = r!p(r), \quad (\text{S37})$$

and

$$G_r^{(r+1)}(x)|_{r \rightarrow \infty} = (r+1)!p(r+1). \quad (\text{S38})$$

By substituting these expressions into the definition of  $k_f(r)$ , we find:

$$k_f(r)|_{r \rightarrow \infty} = (1-f)(r+1) \frac{p(r+1)}{p(r)} = (1-f)H(r). \quad (\text{S39})$$

### Example Class 3: Normal Degree Distribution

For a network with a normal degree distribution:

$$P(k) \sim e^{-\frac{1}{2}\left(\frac{k-\mu}{\sigma}\right)^2}, \quad (\text{S40})$$

we find:

$$H(r) = (r+1) \cdot \exp\left(-\frac{-2r+2\mu-1}{2\sigma^2}\right),$$

and therefore,

$$k_f(r)|_{r \rightarrow \infty} = (1-f)H(r)|_{r \rightarrow \infty} = 0. \quad (\text{S41})$$

### Summary for Random Abandonment

In summary, for random abandonment, the asymptotic behavior of  $k_f(r)$  across the different classes can be expressed as:

$$k_f(r)|_{r \rightarrow \infty} = L(f)H(r) \sim H(r), \quad (\text{S42})$$

where  $H(r) \equiv \frac{P_k(r+1)}{P_k(r)}(r+1)$  and

$$L(f) = \begin{cases} (1-f)/f & \text{if } H(r)|_{r \rightarrow \infty} \rightarrow \infty, \\ (1-f) & \text{if } H(r)|_{r \rightarrow \infty} = H_0. \end{cases} \quad (\text{S43})$$

## 2. $\alpha > 0$ (Preferential Abandonment)

Next, we consider  $k_f$  as a function of  $r$  under preferential abandonment. We have

$$k_f(r) = \frac{\sum_{k'=0}^{\infty} p(k'+r) i_{k'+r} \binom{k'+r}{k'} k' \mu^r (1-\mu)^{k'}}{\sum_{k'=0}^{\infty} p(k'+r) i_{k'+r} \binom{k'+r}{k'} \mu^r (1-\mu)^{k'}} \quad (\text{S44})$$

where  $i_k(f) \sim h^k$  is a function of  $f$  representing the probability that a node of degree  $k$  remains when a fraction  $f$  of nodes has been removed. Here,  $\mu$  is the probability that a neighbor of a node has been removed.

$$\begin{aligned} k_f(r) &= \frac{\sum_{k'=0}^{\infty} p(k'+r) \binom{k'+r}{k'} k' [(1-\mu)h]^{k'}}{\sum_{k'=0}^{\infty} p(k'+r) \binom{k'+r}{k'} [(1-\mu)h]^{k'}} \\ &= \frac{G_r^{(r+1)}(h(1-\mu))}{G_r^{(r)}(h(1-\mu))} h(1-\mu) \end{aligned} \quad (\text{S45})$$

Combining Eq.S7 and Eq.S12, we can have:

$$\mu = \frac{G_1(h)}{h} \frac{1-f}{G_0(h)}. \quad (\text{S46})$$

Since only functions of  $f$  are replaced in this equation, the asymptotic behavior of  $k_f$  depends solely on the network topology.

Therefore, it is easy to obtain:

$$k_f(r) \Big|_{r \rightarrow \infty} = W(h)H(r) \sim H(r), \quad (\text{S47})$$



where

$$W(h) = \begin{cases} \frac{(1-f)G_1(h)}{G_0(h)-(1-f)G_1(h)} & \text{if } H(r)|_{r \rightarrow \infty} \rightarrow \infty, \\ (1-f)G_1(h)/G_0(h) & \text{if } H(r)|_{r \rightarrow \infty} = H_0, \end{cases} \quad (\text{S48})$$

and  $h$  is a function of  $f$ .

we have again:

$$k_f(r)|_{r \rightarrow \infty} \sim H(r) = (r+1) \frac{p(r+1)}{p(r)}. \quad (\text{S49})$$

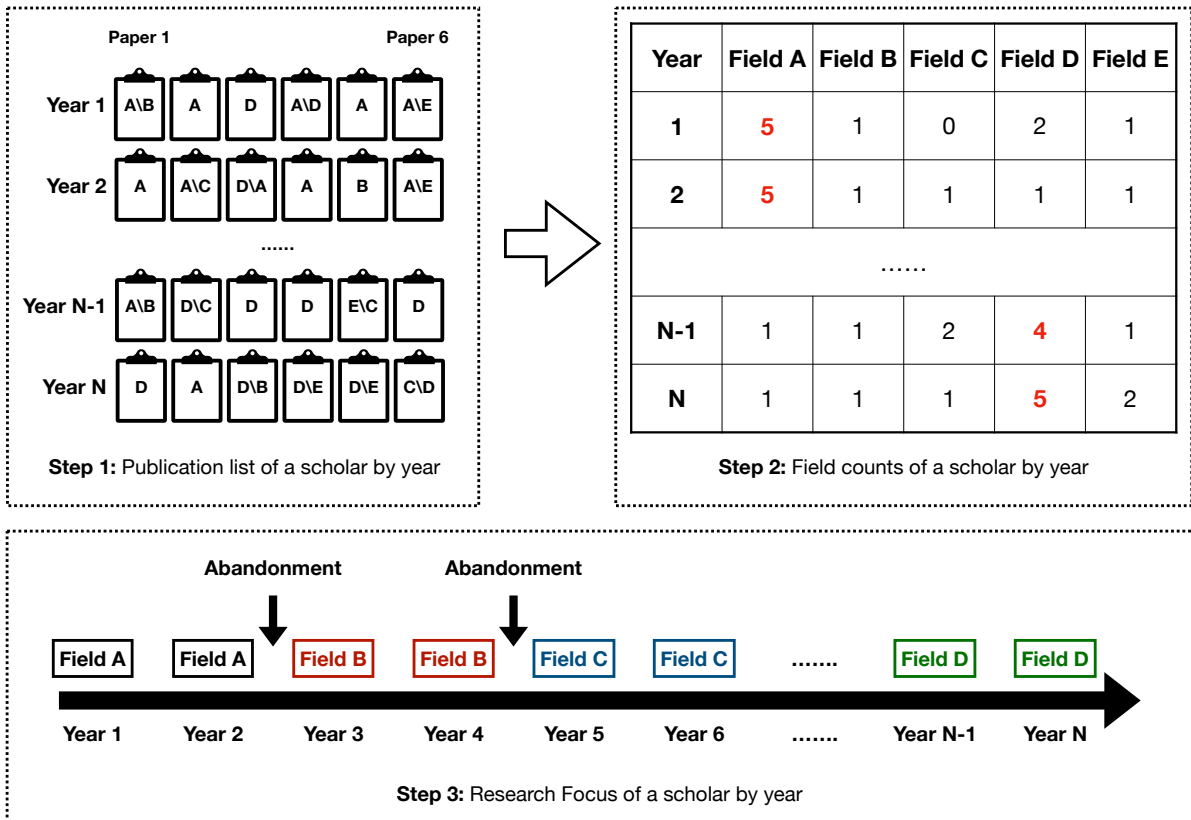


Figure S1: Example of Identifying Field Abandonments for a Scholar.

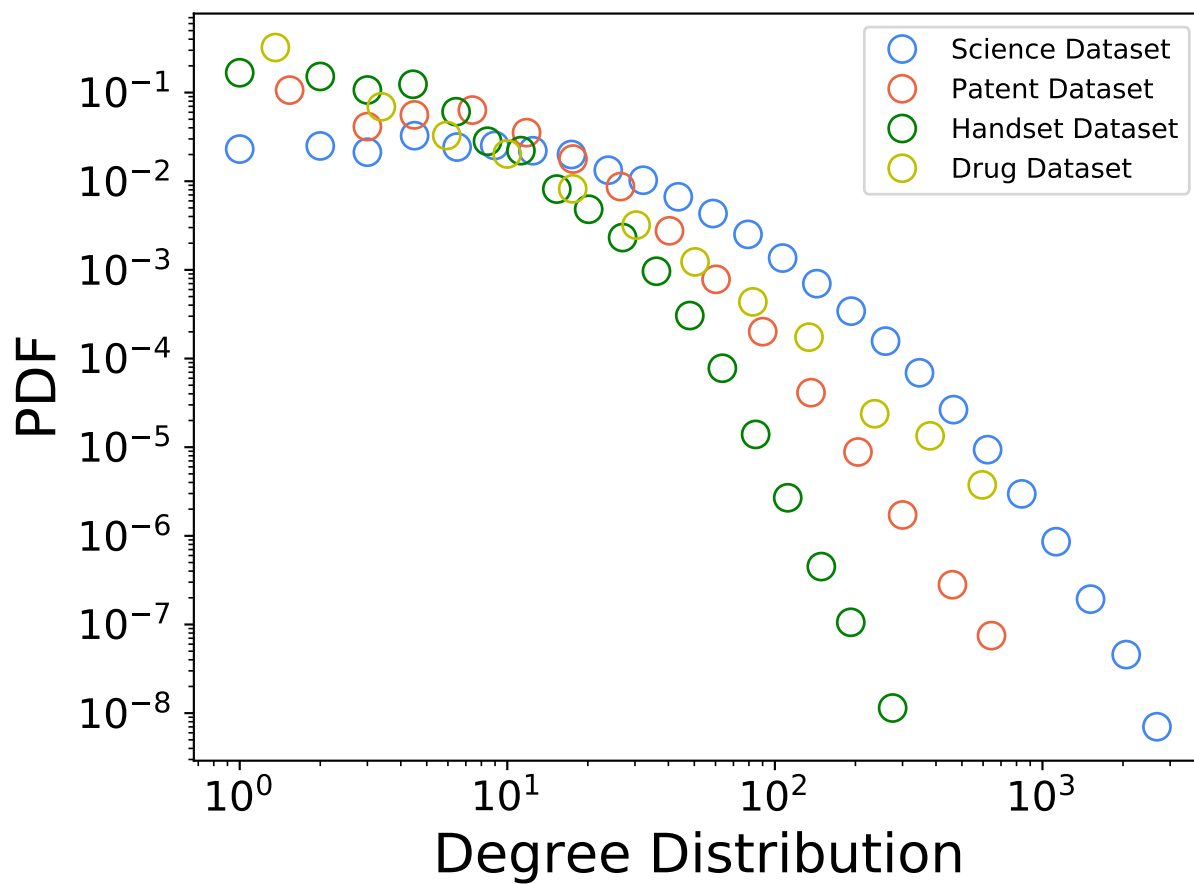


Figure S2: Degree Distribution of the Four Systems.

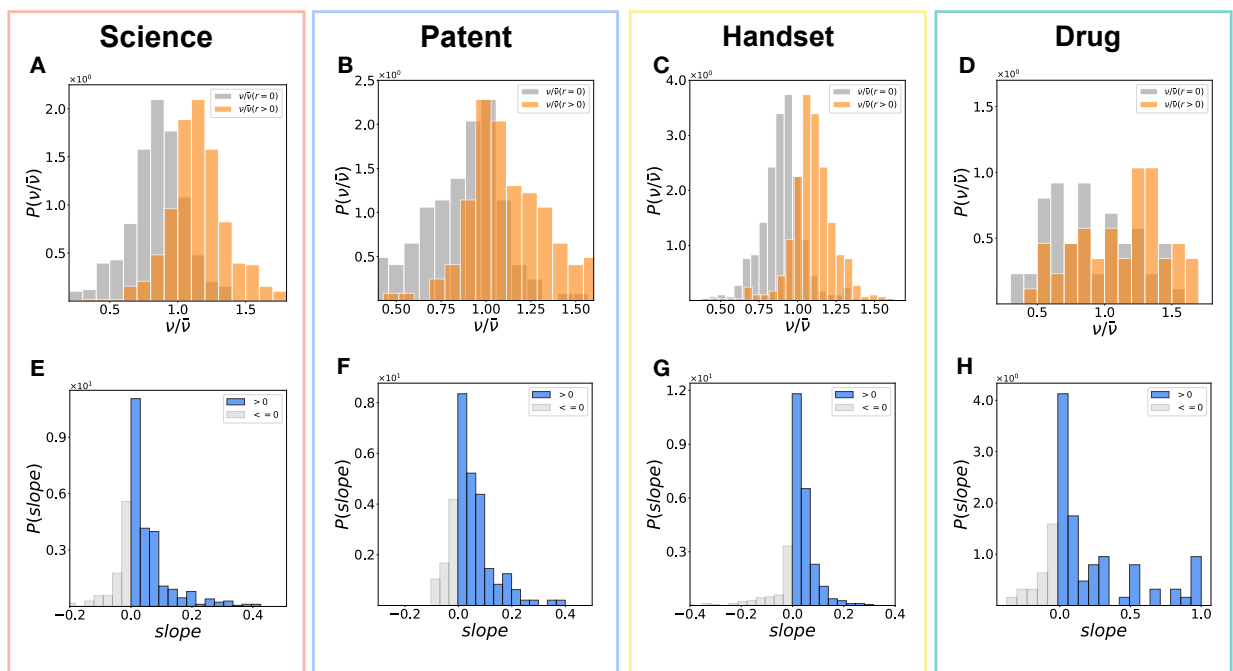


Figure S3: **Robustness Check for Different Time Intervals (Reduced to 60% of Maximum).**

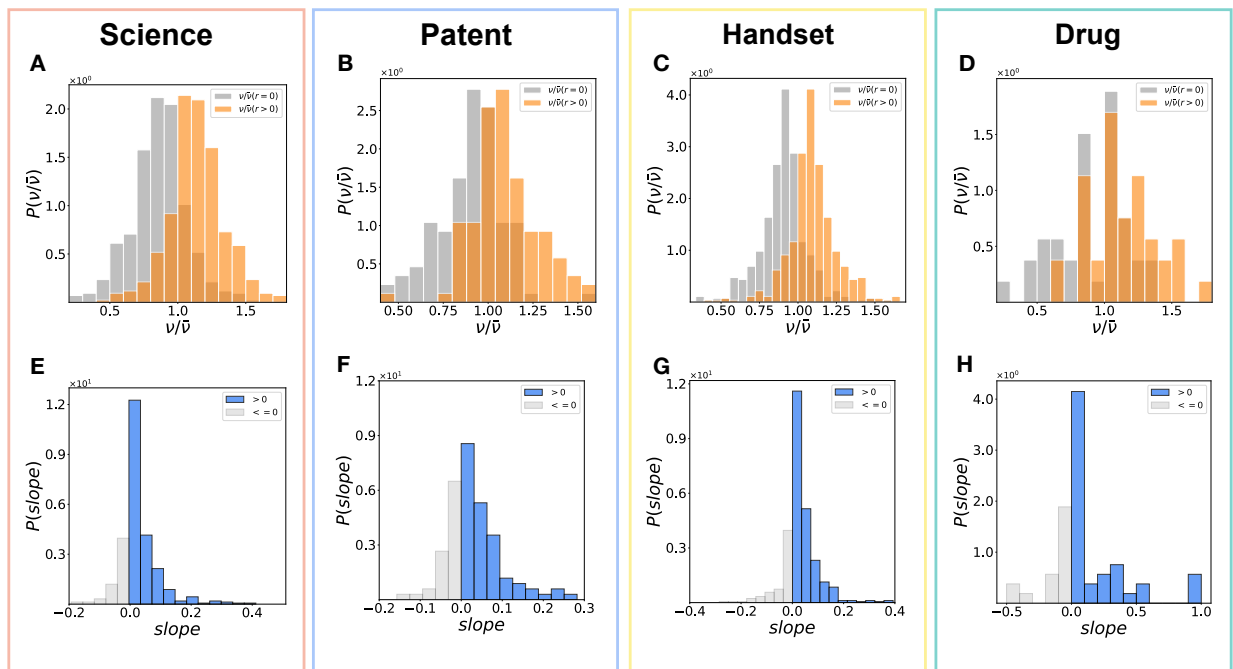


Figure S4: Robustness Check for Different Time Intervals (Reduced to 40% of Maximum).

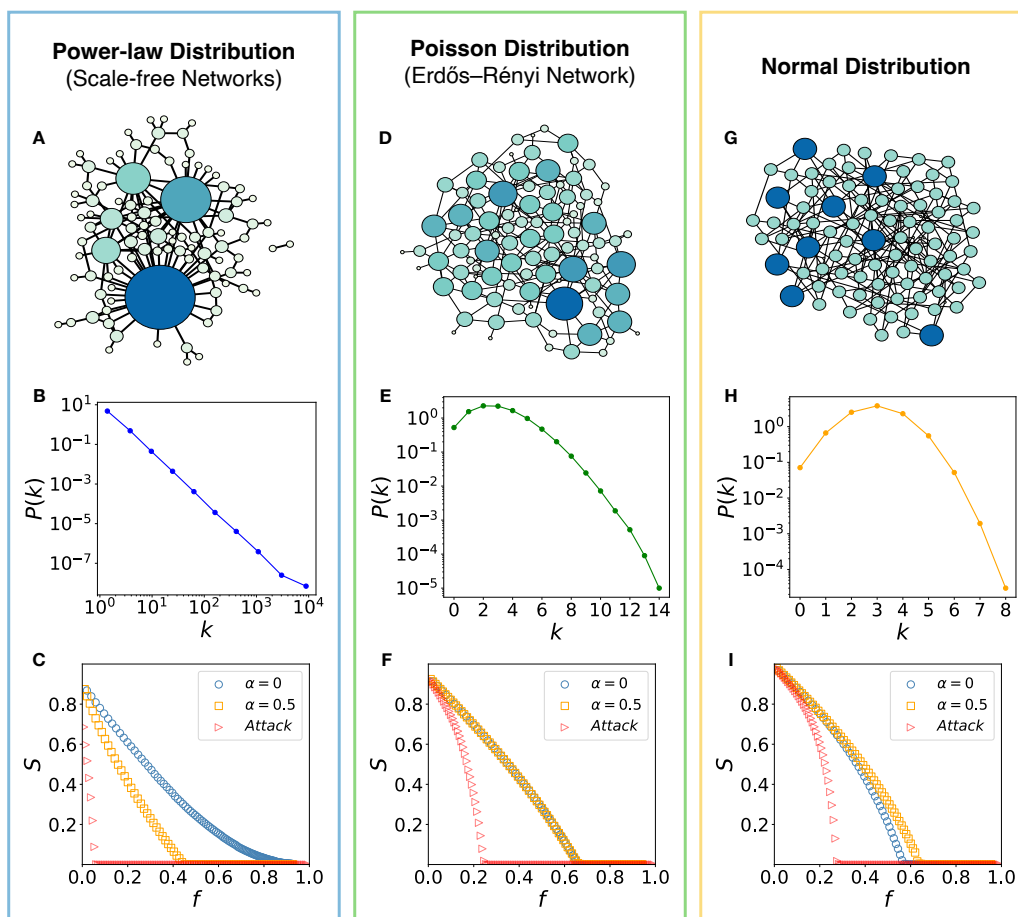


Figure S5: Percolation Process in Different Network Topologies

## S5 Supplementary References

1. Sinha, A. *et al.* An overview of microsoft academic service (mas) and applications. In *Proceedings of the 24th international conference on world wide web*, 243–246 (ACM, 2015).
2. Wang, K. *et al.* Microsoft academic graph: When experts are not enough. *Quantitative Science Studies* **1**, 396–413 (2020).
3. Barabási, A.-L. *Network science* (Cambridge university press, 2016).
4. Pastor-Satorras, R., Castellano, C., Van Mieghem, P. & Vespignani, A. Epidemic processes in complex networks. *Reviews of modern physics* **87**, 925 (2015).
5. Newman, M. *Networks: an introduction* (Oxford University Press, 2010).
6. Molloy, M. & Reed, B. A critical point for random graphs with a given degree sequence. *Random structures & algorithms* **6**, 161–180 (1995).
7. Albert, R., Jeong, H. & Barabási, A.-L. Diameter of the world-wide web. *nature* **401**, 130–131 (1999).
8. Broido, A. D. & Clauset, A. Scale-free networks are rare. *Nature communications* **10**, 1017 (2019).